VISIBLE LASER RESEARCH
ONE METER DEVICE

D. Trainor and H. Hyman
Avco Everett Research Laboratory, Inc.
2385 Revere Beach Parkway
Everett, MA 02149

Interim Technical Report for Period 1 July 1979 to 28 February 1980

Sponsored by

DEFENSE ADVANCED RESEARCH PROJECTS AGENCY
DARPA Order No. 3125

Monitored by

OFFICE OF NAVAL RESEARCH
DEPARTMENT OF THE NAVY
Arlington, VA 22217

FOREWORD

DARPA Order No.: 3125

Contractor: Avco Everett Research Laboratory, Inc.

Effective Date of Contract: August 23, 1976

Contract Expiration Date: February 28, 1979

Contract No.: N00014-76-C-1032

Short Title of Work: One-Meter KrF Laser System

Principal Investigator and Phone No.: D.W. Trainor
(617)389-3000, Ext. 467

Scientific Officer: Director Physics Program
Physical Science Division
Office of Naval Research
800 North Quincy Street
Arlington, VA 22217

Amount of Contract: $1,778,190

UNCLASSIFIED

SECURITY CLASSIFICATION OF THIS PAGE *(When Data Entered)*

REPORT DOCUMENTATION PAGE	READ INSTRUCTIONS BEFORE COMPLETING FORM
1 REPORT NUMBER	2. GOVT ACCESSION NO. AD-A084 794	3. RECIPIENT'S CATALOG NUMBER
4. TITLE *(and Subtitle)* VISIBLE LASER RESEARCH ONE METER DEVICE	5. TYPE OF REPORT & PERIOD COVERED Interim ~~Technical~~ Report 1 Jul 1979 - 28 Feb 1980
	6. PERFORMING ORG. REPORT NUMBER
7. AUTHOR(s) D. Trainor [redacted] H. Hyman	8. CONTRACT OR GRANT NUMBER(s) N0014-76-C-1032, DARPA Order-3125
9. PERFORMING ORGANIZATION NAME AND ADDRESS Avco Everett Research Laboratory, Inc. 2385 Revere Beach Parkway Everett, MA 02149	10. PROGRAM ELEMENT, PROJECT, TASK AREA & WORK UNIT NUMBERS 61102F 2308
11. CONTROLLING OFFICE NAME AND ADDRESS Defense Advanced Research Projects Agency DARPA Order No. 3125	12. REPORT DATE
	13. NUMBER OF PAGES 49
14 MONITORING AGENCY NAME & ADDRESS *(If different from Controlling Office)* Office of Naval Research Depdrtment of the Navy Arlington, VA 22217	15. SECURITY CLASS. *(of this report)* Unclassified
	15a. DECLASSIFICATION/DOWNGRADING SCHEDULE

16. DISTRIBUTION STATEMENT *(of this Report)*

Approved for public release; distribution unlimited.

17. DISTRIBUTION STATEMENT *(of the abstract entered in Block 20, if different from Report)*

18. SUPPLEMENTARY NOTES

19. KEY WORDS *(Continue on reverse side if necessary and identify by block number)*

Blue-Green Lasers
Stimulated Raman Scattering
XeF*
Hydrogen
Deuterium
lambda

20. ABSTRACT *(Continue on reverse side if necessary and identify by block number)*

Stimulated Raman Scattering Experimental Results are discussed. The pump laser was XeF (λ = 350 nm) and two step conversion to the blue-green spectral region was accomplished using molecular hydrogen and deuterium. Conversion efficiencies were measured and overall conversion from the UV to the blue-green of >40% is reasonable.

DD FORM 1 JAN 73 1473 EDITION OF 1 NOV 65 IS OBSOLETE

UNCLASSIFIED 048450

SECURITY CLASSIFICATION OF THIS PAGE *(When Data Entered)*

TABLE OF CONTENTS

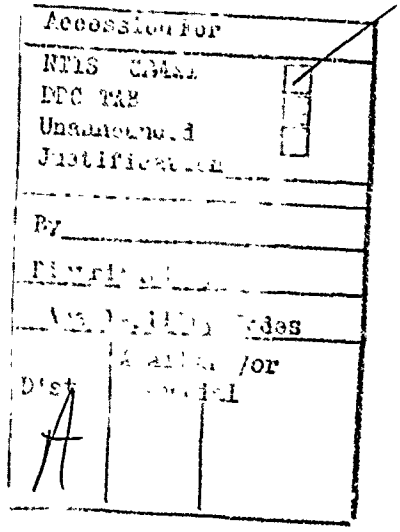

LIST OF ILLUSTRATIONS

I. INTRODUCTION

There is an ongoing need in a variety of Department of Defense applications for a dependable, efficient, high average power laser operating at ocean water transmitting wavelengths ($\lambda \cong 470$ nm). It has also been historically true that few lasers operating near this optimal wavelength are available, let alone meet the requirements for efficient, scalable operation. To develop a blue-green laser system, one can either explore new laser concepts leading to direct lasing in this sought-after bandpass or undertake means to shift the output wavelength of existing, proven lasers into the desired regime. One such class of proven lasers are the exciplex lasers which include the rare gas halides, halogens and mercury halides (see Table I). Of these exciplex systems, there are four that have a demonstrated capacity for respectable efficiencies and scalable, high power operation; namely ArF* (193 nm), KrF* (249 nm), XeCl* (308 nm) and XeF* (351 nm). Of these, we feel XeF* shows the most promise as a basis for an efficient converter. This is based principally on its suitability for scaling to high power and the fact that the blue-green spectral region can be readily accessed by stimulated Raman output from XeF* pumped molecular hydrogen.

For any stimulated Raman process phenomenologically, the acceptor molecule (e.g., H_2) can be thought of as absorbing an incident photon (e.g., XeF* 351 nm) thereby making a transition to a virtual state and then, with the emission of a Raman photon at longer wavelengths, proceeding to a level near the ground (initial) state (e.g., H_2 (v = 1)). Stimulated Raman scattering in hydrogen by rare gas halide pumps has been studied at LASL.[1] The forward scattering cross section is large and overall energy conversion efficiency of ~ 80% has been observed with $\gtrsim$ 50% in the 1st Stokes line routinely reported.(1)

TABLE I

A SUMMARY OF EXCIPLEX LASERS AND THEIR LASING WAVELENGTHS

EXCIPLEX	$\lambda (B \rightarrow X)$ nm
ArF	193
KrCl	222
KrF	249
XeBr	282
XeCl	308
XeF	351 ($B \rightarrow X$), 500 ($C \rightarrow A$)
F_2	158
FCl	284
Br_2	292
I_2	342
IF	491
HgI	440
HgBr	502
HgCl	558

J4217

We have been experimentally investigating wavelength conversion of XeF* to the blue-green using this technique of stimulated Raman scattering involving hydrogen and deuterium.

In particular, our approach involves sequential conversion through two distinct, separate steps involving H_2 and D_2:

Step 1

$$h\nu_{XeF} + H_2(\text{1st Stokes}) \rightarrow h\nu_{H_2}\ (411,414\ \text{nm})$$

Step 2

$$h\nu_{H_2}(411,414\ \text{nm}) + D_2(\text{1st Stokes}) \rightarrow h\nu_{output}(469,472\ \text{nm})$$

The use of two separate cells provides wavelength flexibility through the choice of appropriate Raman scattering media in the various cells. In addition, optimization on first Stokes in both cells, sequentially, each in a single pass, is a straightforward method for minimizing the effects of four-wave, parametric mixing processes which can reduce the desired Stokes output.

The ability of the AERL two-step approach to select a desired wavelength through the choice of the gases contained in the two cells can have significant system advantages, since various ocean water types have different wavelength transmission properties (see Figures 1-5). Figure 1 shows the Jerlov attenuation coefficients as measured through the top 10 m of surface water classified according to ocean types. Figure 2 plots the same data as attenuation of incident light through 100 m of ocean water, assuming the top 10 m are characteristic of the entire optical path length. For types I, II and III water, there is a clear advantage in transmitted signal for wavelengths near 475 nm, and a laser operating at or near this wavelength would be appropriate for all three ocean types. For coastal types, longer wavelength lasers offer some advantage but the extreme signal attenuations involved may suggest that wavelength may not be the single most significant issue.

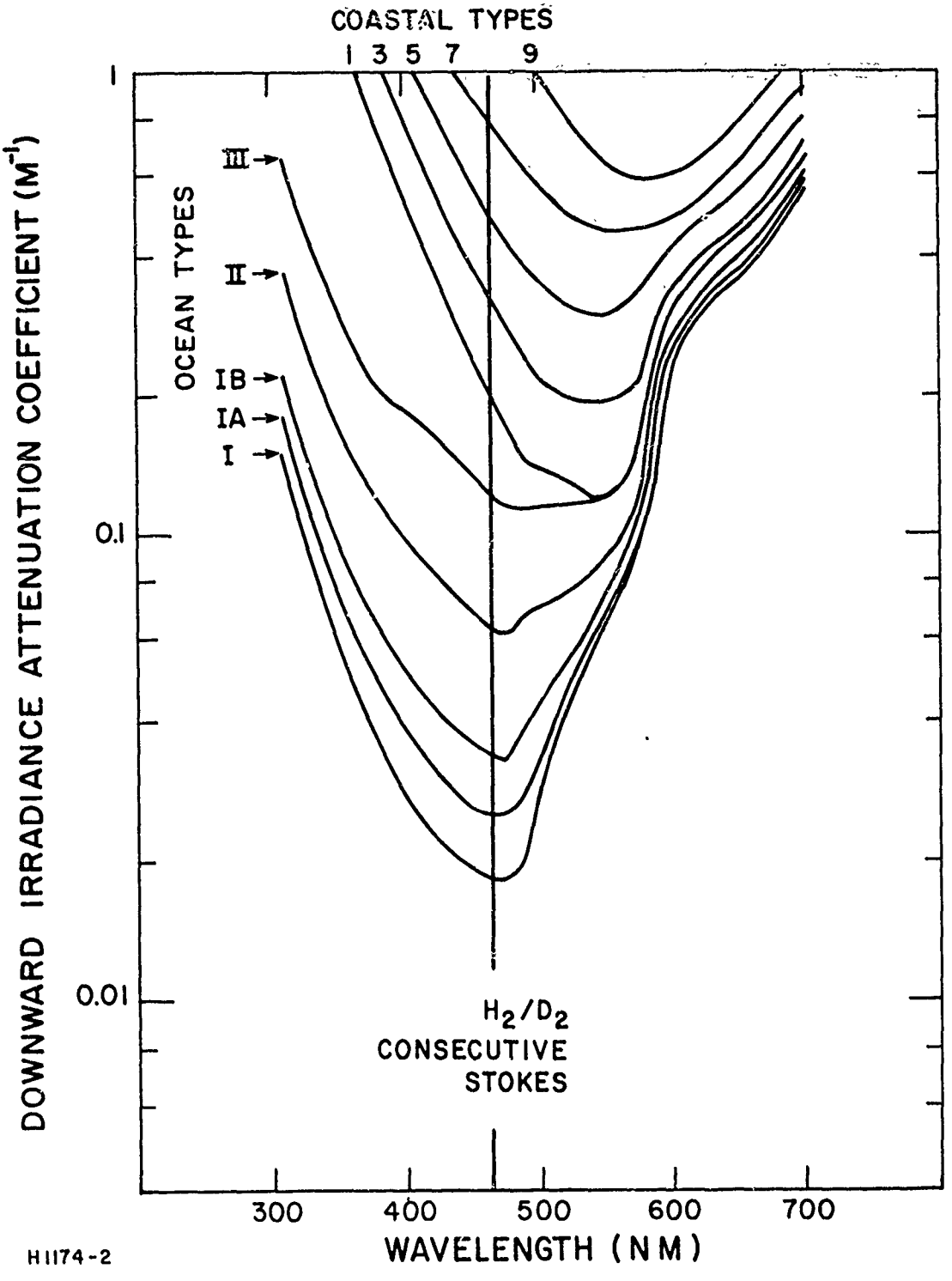

Figure 1 Ocean Water Attenuation Coefficients vs Wavelength Indicating XeF* Raman Conversion Wavelength

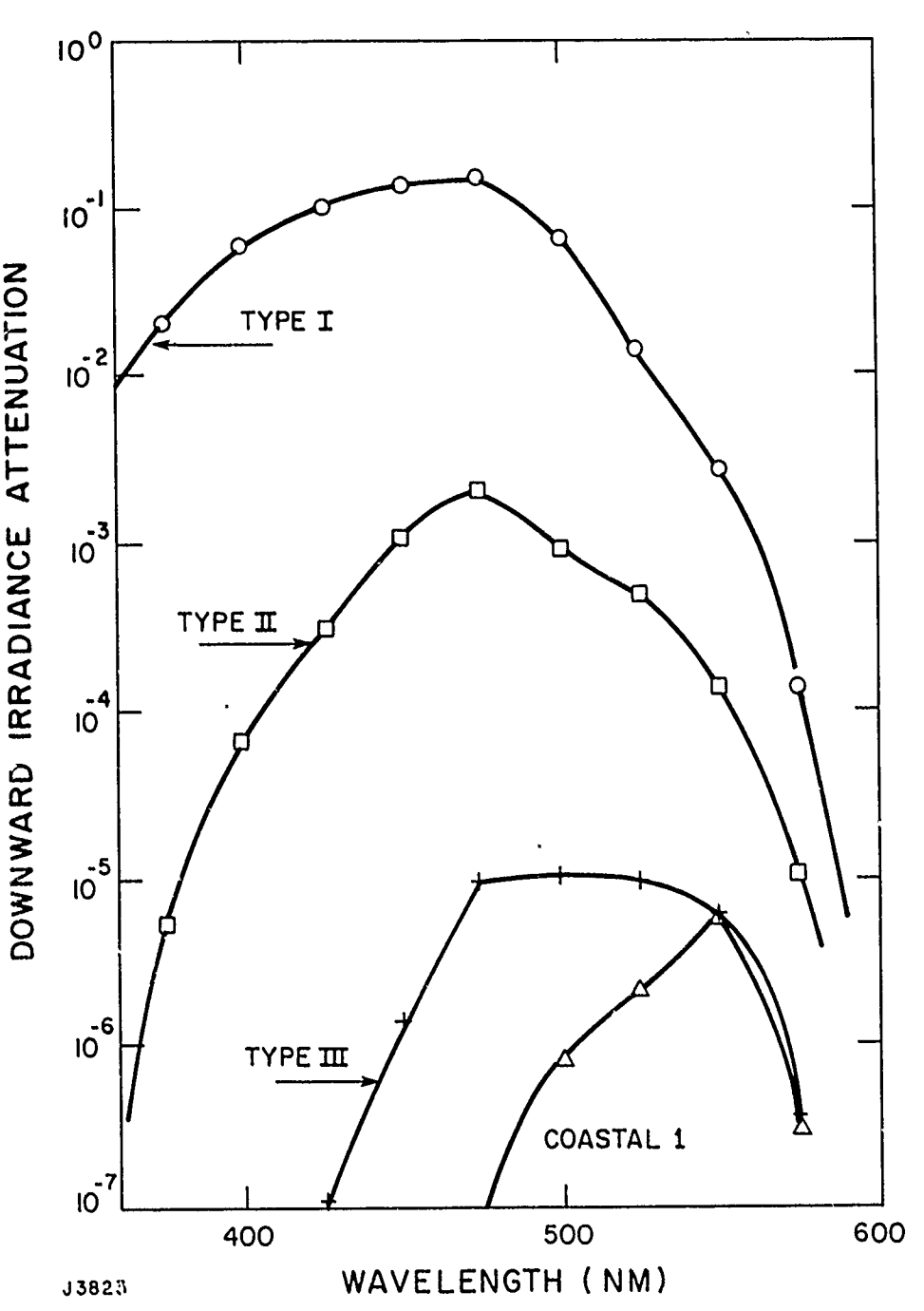

Figure 2 Downward Irradiance Attenuation vs Wavelength

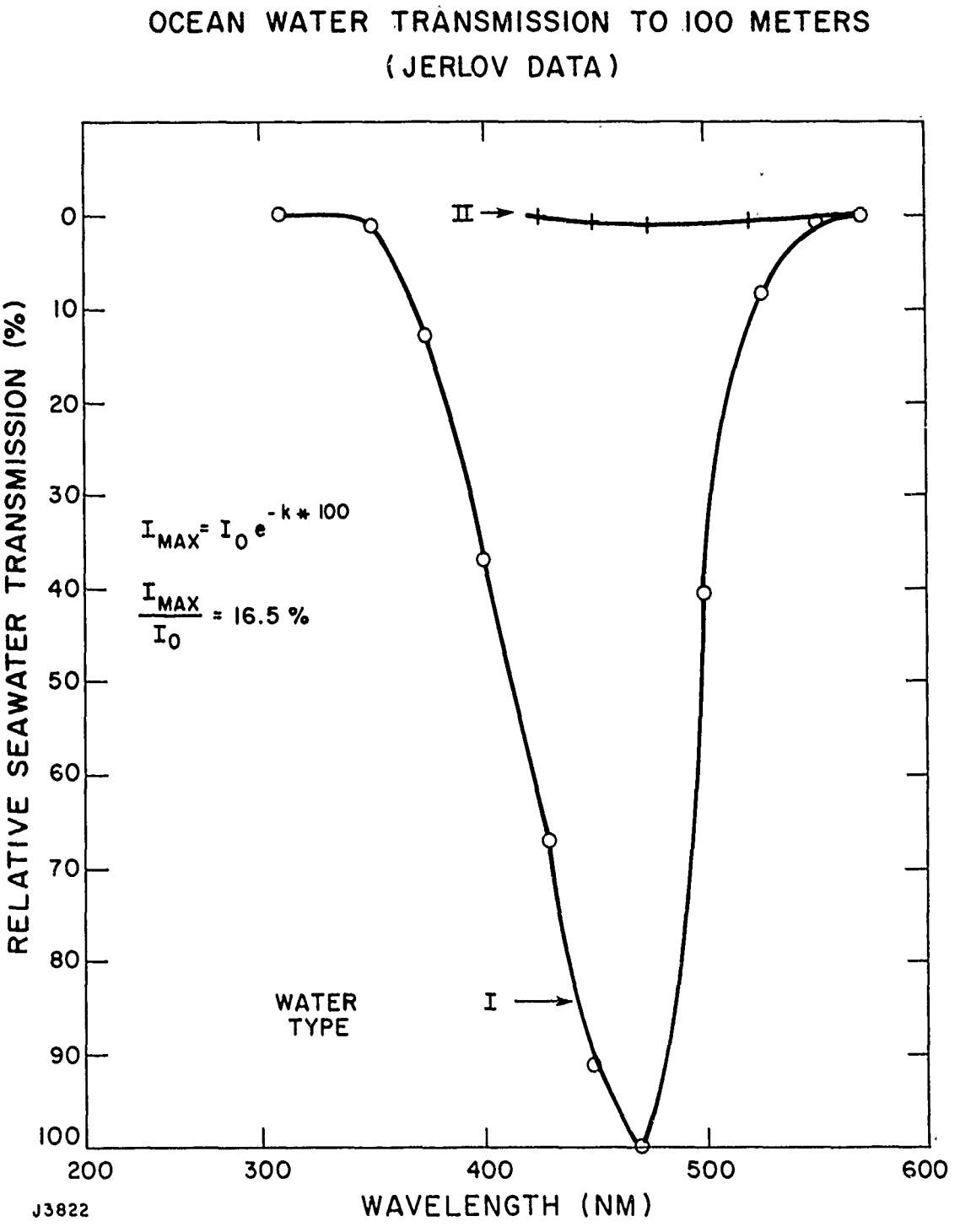

Figure 3 Relative Seawater Transmission vs Wavelength for Water Types I and II

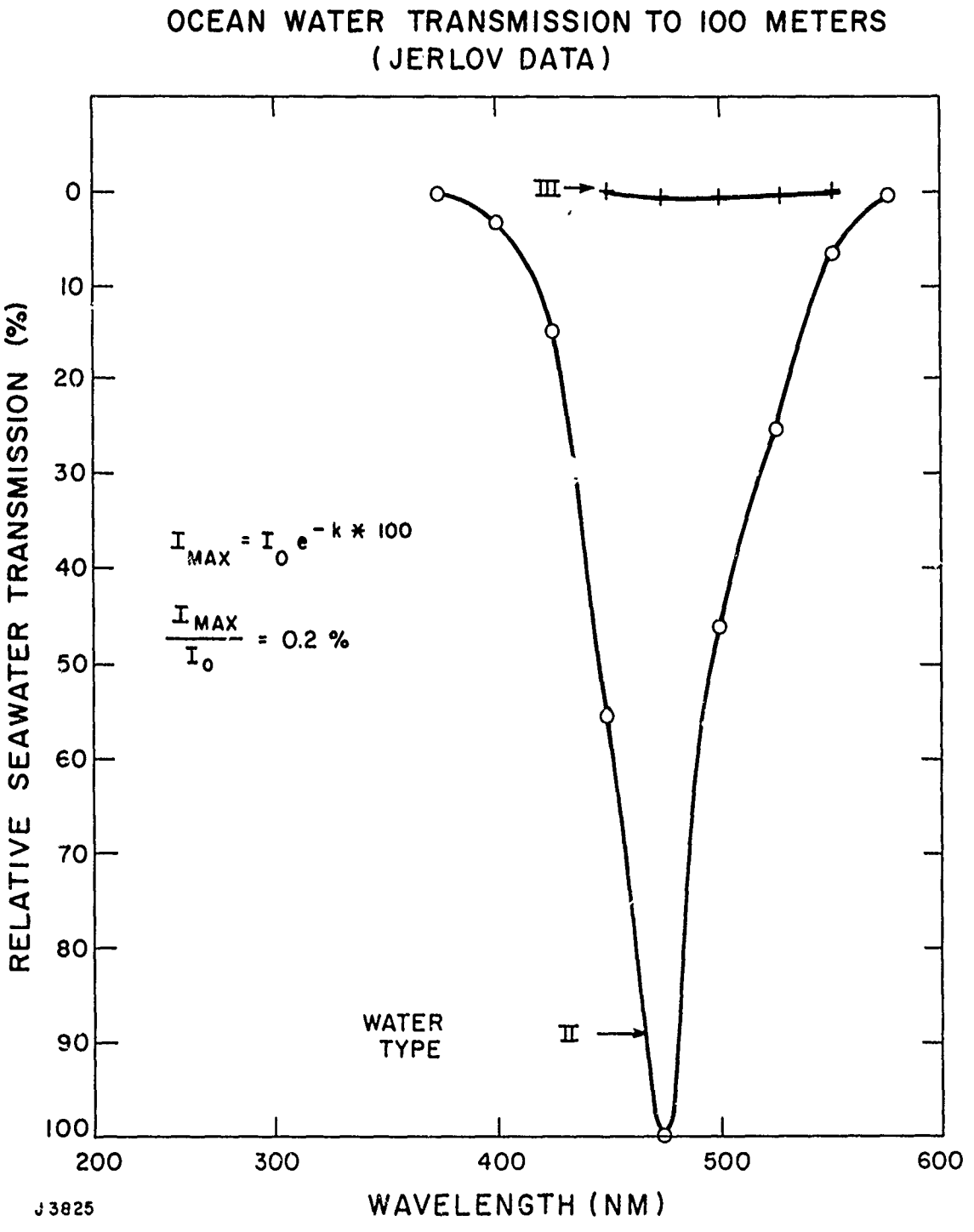

Figure 4 Relative Seawater Transmission vs Wavelength for Water Types II and III

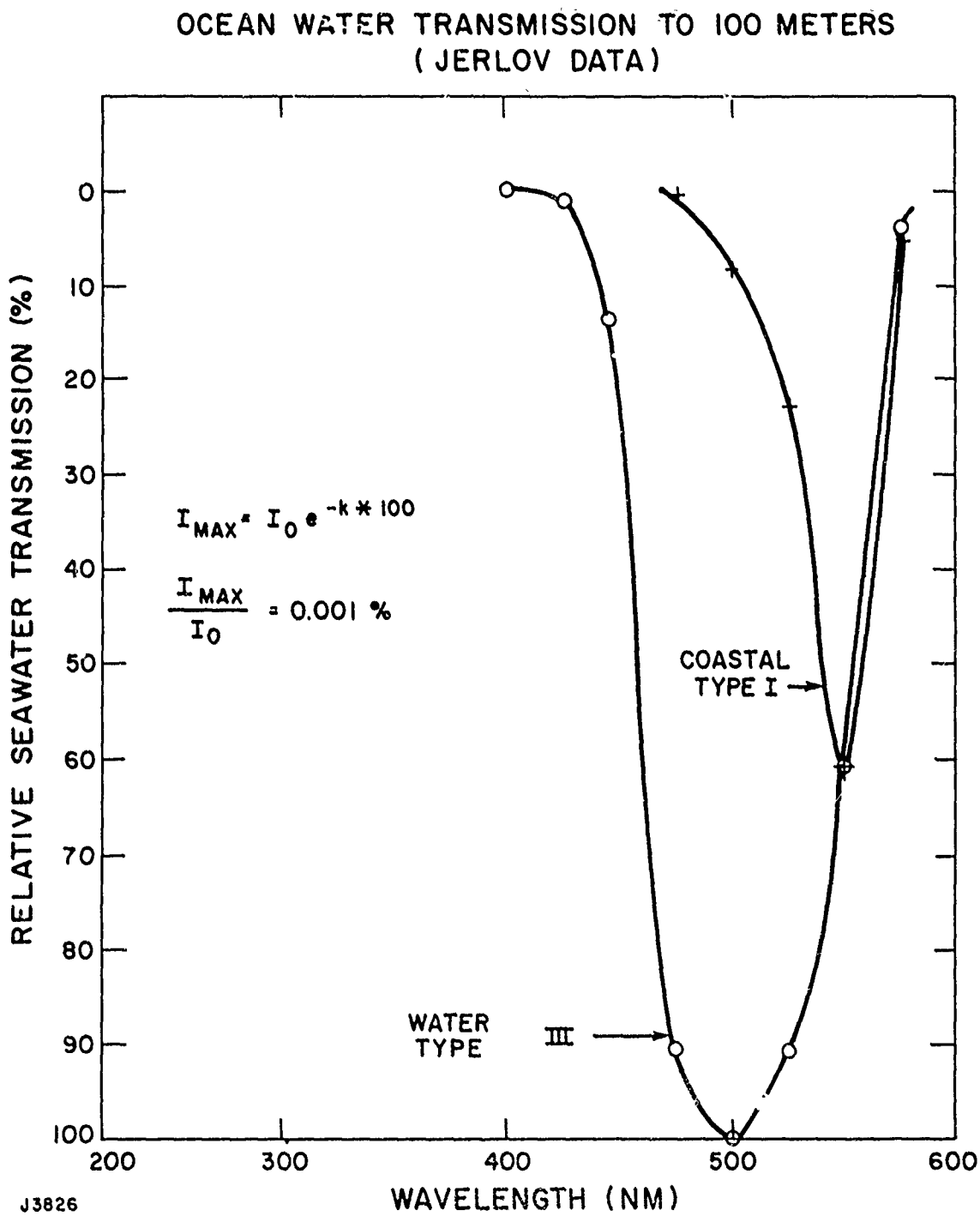

Figure 5 Relative Seawater Transmission vs Wavelength for Water Type III and Coastal Type 1

This influence of wavelength is depicted on a relative basis in Figures 3-5. Here the peak transmission is listed for the optimum wavelength along with a plot of the relative wavelength scaling for each ocean type normalized to the peak. For example, Figure 4 shows maximum 100 m transmission through ocean type II is 0.2% at 475 nm. At this same wavelength, type III transmits a very small percentage (see top of Figure 4) and itself is plotted with coastal type 1 in Figure 5. These graphs, which plot transmission on a linear scale, demonstrate more clearly the significant dependence of the transmitted signal on wavelength.

Blue-green lasers operating as near to the ocean transmission window as possible provide the greatest potential signal-to-target, thus reducing the required laser power needed to provide any minimally acceptable receiver signal. The output wavelengths of 469 and 472 nm, corresponding to our approach of two-step conversion with D_2 and H_2 of the two lasing transitions of XeF*, are nearly optimum for ocean water transmission based on these Jerlov data. Since high conversion efficiency has been demonstrated in H_2 at AERL with an XeF* laser pump, we project that, starting with an XeF* overall efficiency of $\geq 4\%$, an overall blue-green laser efficiency of $\geq 1\%$ is attainable.

II. BACKGROUND

In general, for the stimulated Raman process both atomic and molecular gases can act as the nonlinear medium, and some of the differences between the atomic and molecular cases are illustrated in Figure 6. For any stimulated Raman process, the acceptor atom or molecule can be thought of as absorbing an incident photon (e.g., XeF* 351 nm) thereby making a transition to a virtual state and then, with the emission of a Raman photon at longer wavelengths, proceeding to a level near the ground (initial) state. For an atomic candidate, the practical constraints involve searching for an atom which has a dipole allowed electronic transition near the pump laser frequency and a corresponding transition from that upper state (2) to a lower state (3) at the sought-after conversion wavelengths. Specifically, for this blue-green mission, workers at the Naval Research Laboratory (Ref. 2) have reported high conversion efficiency of XeCl (308 nm) to 459 nm using atomic lead as the scattering candidate. These atomic systems do, however, have the singular disadvantage of requiring high-temperature production techniques (heat pipes) which may prove technologically difficult at the very high average powers under consideration for actual systems applications. In addition, the typical achievable metal atom density requires the use of the metal atom more than once during the laser pulse (recycling) or large volume sources, since one must have at least as many metal atoms as photons for high conversion efficiency. For molecular Raman scattering (see Figure 6), the process is generally the same as in the atomic case but is much more non-resonant. Since there is no resonant enhancement of the cross section, large densities are usually required to produce reasonable gain for readily available pump lasers.

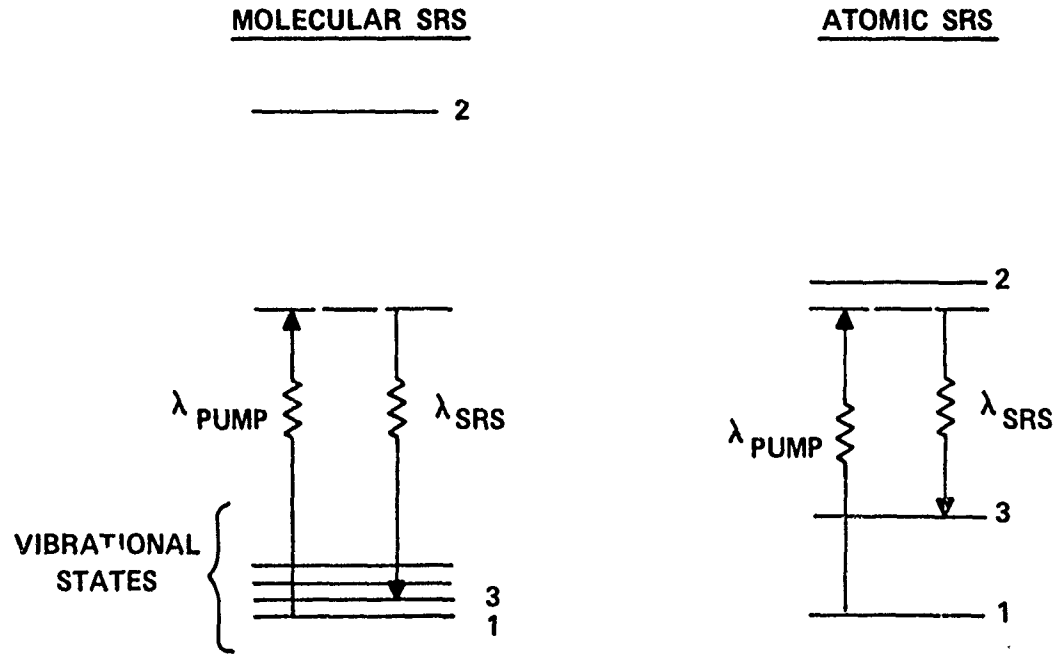

Figure 6 Optical Conversion by Stimulated Raman Scattering

III. RESULTS

A. SHORT-PULSE LASER RESULTS

For the past eight months, we have been investigating efficient generation of Stokes shifted radiation using a commercial exciplex laser as the pump (Lumonics, TE-261-2) and molecular H_2 and D_2 as the Raman scattering media. General laser specifications as detailed by the manufacturer were found to be achievable with our particular device (e.g., it produced $\sim$75 mJ of energy per pulse with XeF* and $\sim$190 mJ for KrF* with the cavity optics provided). The beam quality associated with these achievable energies was insufficient to provide focussed intensity-length products to achieve laser action in the Raman gas. We, therefore, altered the cavity optics to include Brewster windows and an unstable cavity configuration of the type described by Barker and Loree (Ref. 3). This cavity produced $\lesssim$ 20 mJ of XeF laser energy in a pulse (FWHM) of $\simeq$ 6 ns with a beam waist 10 times the diffraction limited value. The power density achievable was measured at the focus by recording the energy transmitted through various diameter pinholes. The beam waist at the focus of a 50 cm fl lens was found to be near 2.5×10^{-2} cm in diameter with an energy of 10 mJ. This, with the 6 ns pulselength, corresponds to an achievable power density of $\sim 3 \times 10^{9}$ W/cm^2 at the focus.

Efficient conversion however relies on an intensity-density-length product well in excess of threshold to achieve optimum conversion of XeF pump radiation to first Stokes. To measure efficiency and to parameterize the Raman process, the experimental setup shown in Figure 7 was used. Here the output of the Lumonics was focussed through a pinhole to 1) characterize the input beam, and 2) eliminate that portion of the pump with poor beam quality. In this arrangement, a second lens refocusses the beam into the center of our high-pressure Raman cell.

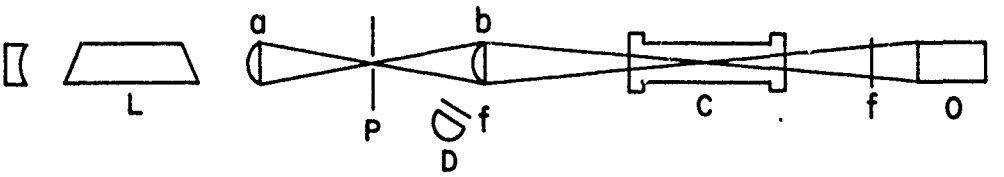

Figure 7 Schematic of Experimental Setup where L is the Lumonics Laser, a and b are 50 cm fL lens, C is the High-Pressure Cell, D is a Photodiode, F are Filters and O is a Spectral Monitoring or Energy Measuring Device

The Raman cells were constructed from available stainless steel shock tube sections about 40.6 cm long with an inner diameter of 3.8 cm and a wall thickness near 1.3 cm. The polished Ultrasil quartz windows were near 6 cm in diameter and ~ 2.5 cm thick. The windows were supported by O-rings on the high-pressure side and by gaskets on the low-pressure side. The internal volume of these cells was near 465 cm^3.

Pulse energies in these experiments were measured with a Scientech Model 362 energy/power meter. Pulse shapes were measured by photodiodes (ITT, type S-5 or Hammamatsu, type S-4). The outputs from the photodiodes were recorded by a Tektronics Model 7844 dual beam oscilloscope equipped with a C-51 oscilloscope camera.

Spectra were analyzed with either a 3/4 m monochromator, 1 m spectrograph, or an optical multichannel analyzer (Tracor Northern, Model TN-1710, equipped with a Diode Array Rapid Scan Spectrometer).

Using this arrangement and these various diagnostics, the effects of laser intensity, focal length, and H_2 pressure on the stimulated Raman scattering threshold, gain, Stokes production and conversion efficiency were investigated.

The pump laser intensity (at fixed focal length) was varied in two ways: by repeated firings to degrade the mix from optimum or by lowering the laser charging voltage. Using either technique, the subsequent results were identical, so the more convenient technique of varying the charging voltage was usually employed. Since these experiments were all carried out with focussed geometry, a related factor to the intensity achieved (W/cm^2) is the length over which the intensity was high. A visual perspective of the various focal arrangements used is shown in Figure 8. These pictures were obtained by open shutter exposures of the focussed laser light into a glass

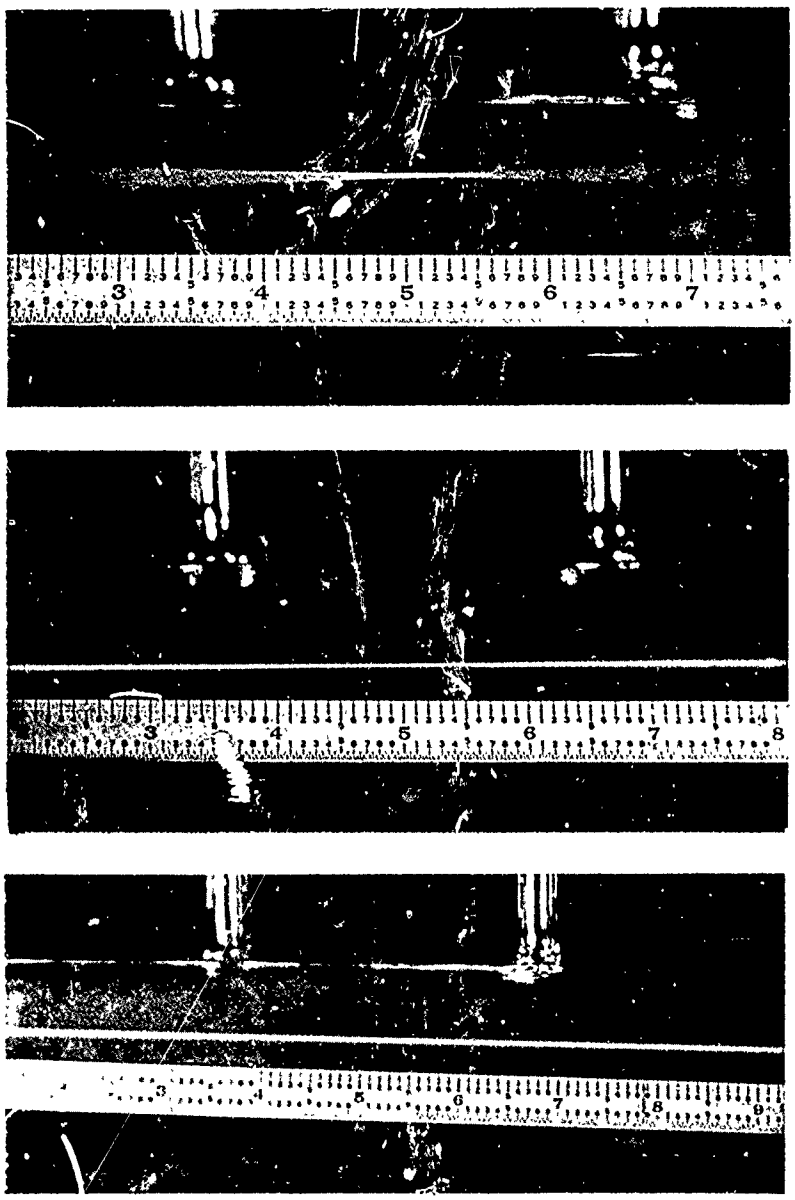

Figure 8 Focal Length Profiles

cell containing a dilute solution of Rhodamine 6G. The focal length of ~ 135 cm geometry provided a beam waist of about 0.05 cm in diameter. Figure 9 shows a plot of the energy through this size pinhole vs distance from focus. The distance beween half-power points (or the effective Rayleigh range) is about 8 cm. Since the active length of the high-pressure cell is over 40 cm, there was no problem anticipated with gain clipping and no effect on the Raman output was observed when a Raman cell of ~ 90 cm was used.

For this experimental setup (at a maximum laser output corresponding to near 4.5×10^8 W/cm^2 for this relatively soft focal geometry), the dependence on forward scattered Stokes generation on H_2 pressure was measured (see Figure 10), using the optical multichannel analyzer (note that the intensity vs wavelength calibration has not been measured). The first Stokes component appears to optimize at pressures above 15-20 atms (~ 250 psi) whereas the second Stokes appears to peak near 25-30 atm and then decrease at higher pressures. These pressure scaling results are in agreement with the KrF/H_2 experiments of Loree (Ref. 1) and the gain saturation reported by Bloembergen (Ref. 4).

By now keeping the focal length and H_2 pressure fixed, variations in Stokes output were measured as a function of XeF pump input, (see Figure 11). With data similar to these, it is possible to calculate the small-signal gain for this single step process. From our measurements, we found threshold to be near 2.2 mJ. The pulsewidth was 6 ns and the length over which significant conversion occured was near 8 cm with a beam waist at the center of the focal region of ~ 0.05 cm. Since it is commonly regarded that a gain times length ~ 30 is necessary to achieve lasing from noise (i.e., spontaneous Raman scattering), we can calculate the small-signal gain, g, as follows:

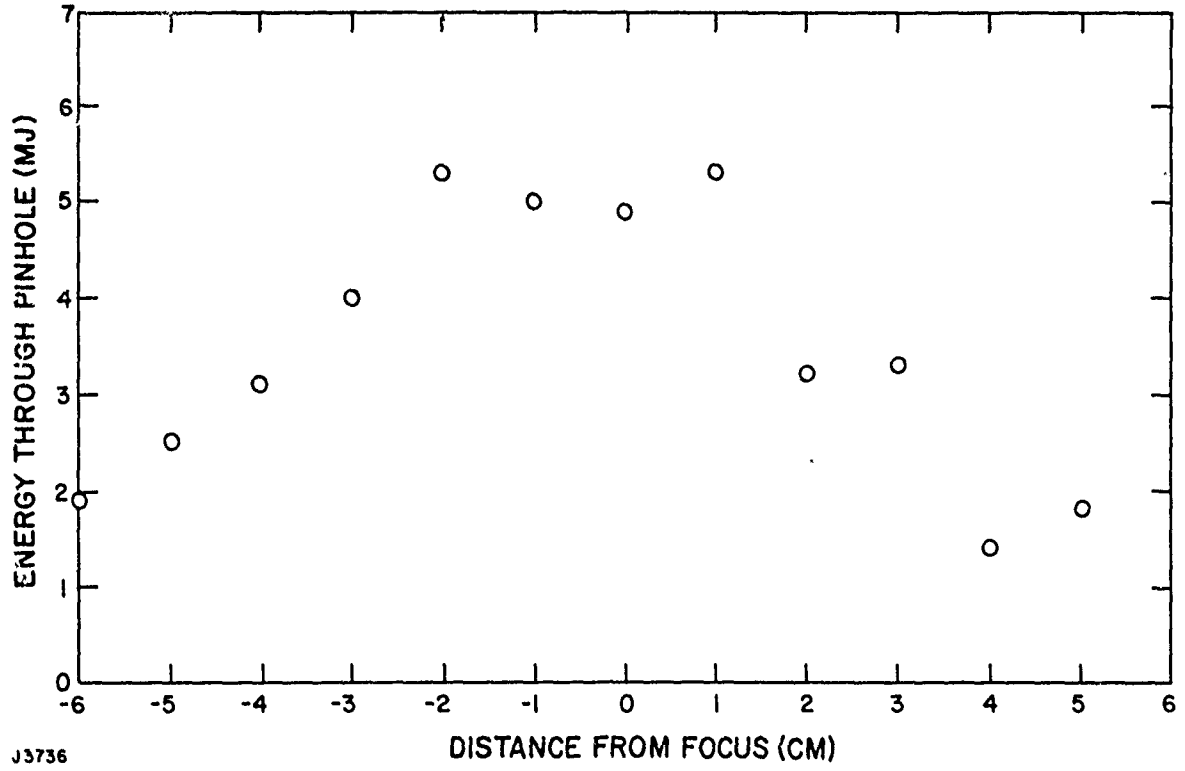

Figure 9 Energy Measured Through a 0.05 cm Pinhole vs Distance from Focus

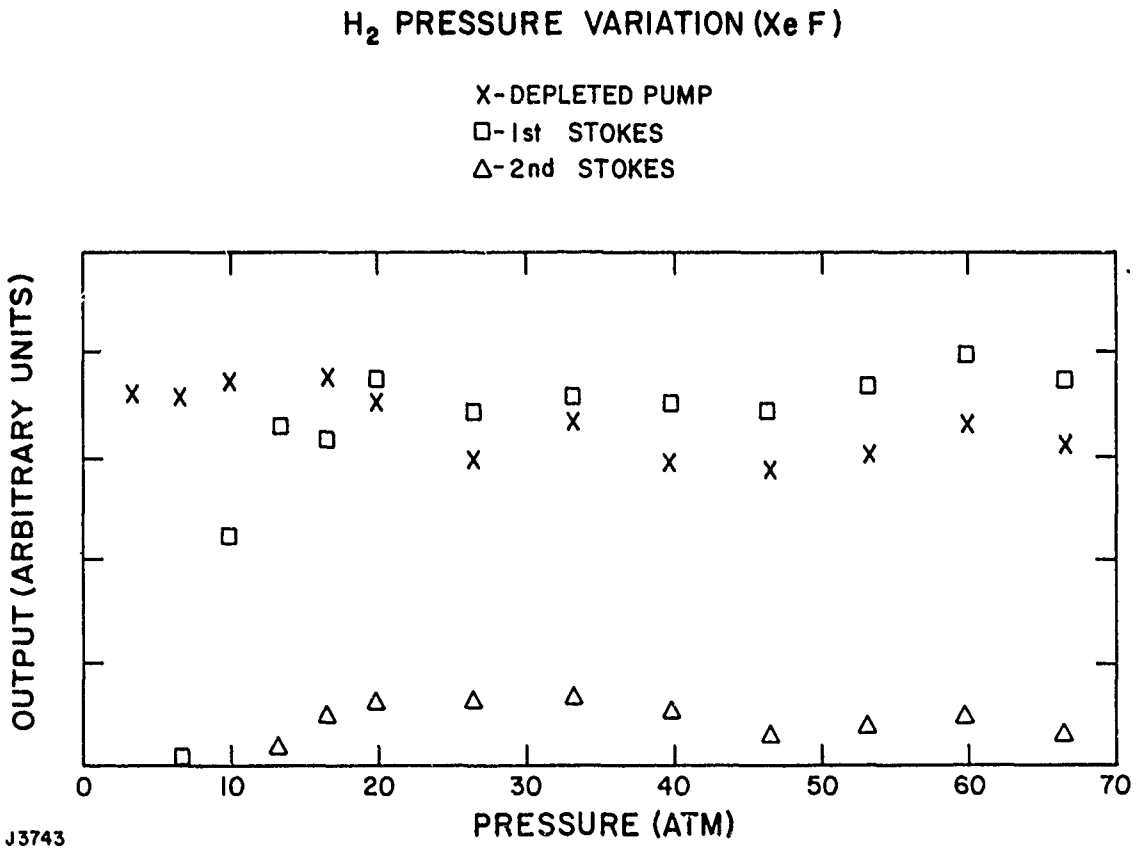

Figure 10 Various Laser Output Photons vs Total H_2 Pressure

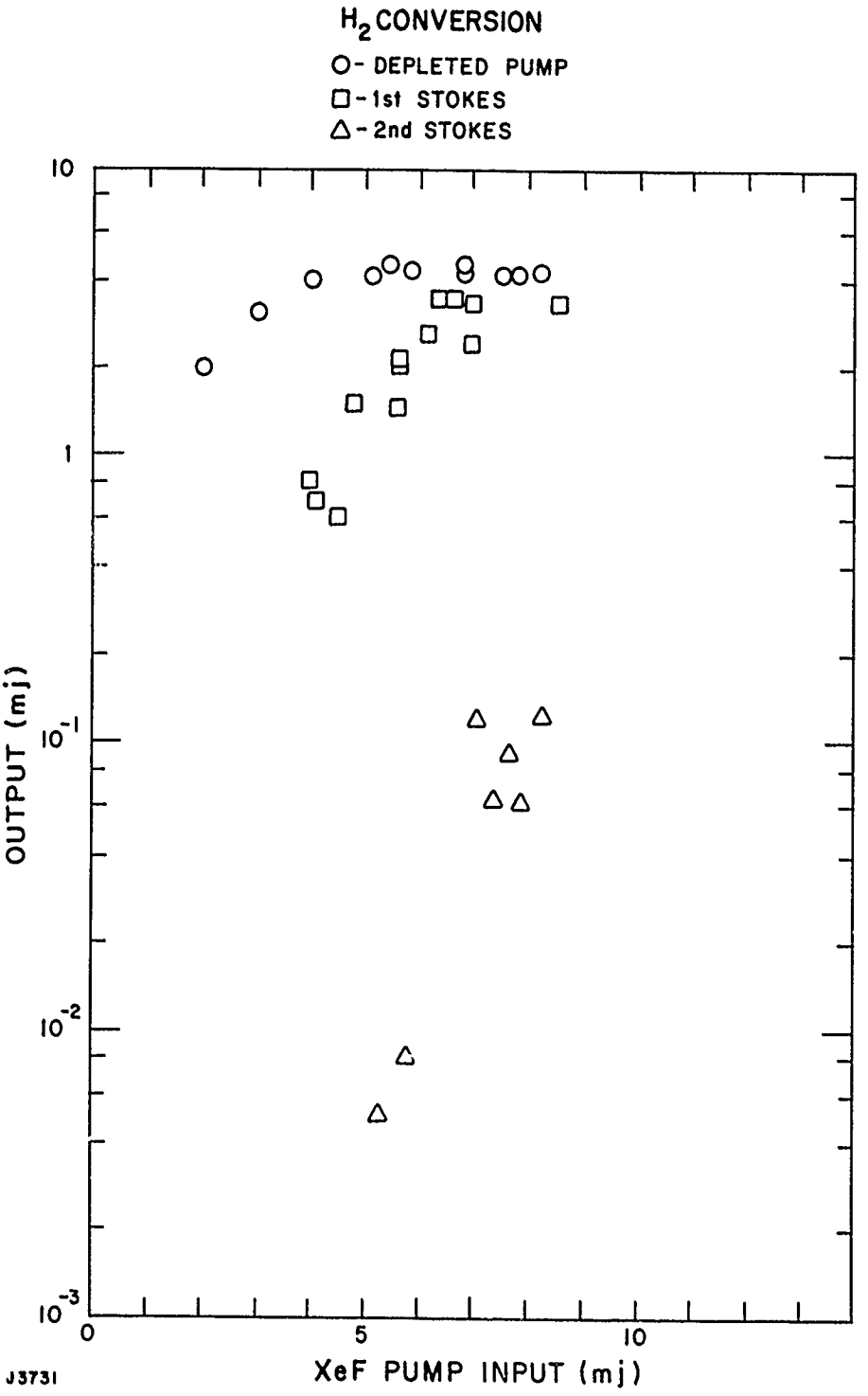

Figure 11 Optimized XeF Conversion to First Stokes vs Input Energy

$$g\ I_{Th}\ L \sim 30$$

where

$$I_{Th} = \frac{2.2 \times 10^{-3}\ J}{6 \times 10^{-9}\ s \times \pi\ (0.025\ cm)^2} = 1.9 \times 10^8\ \frac{W}{cm^2},$$

and L = 8 cm

$$\therefore g \lesssim \frac{30}{I_{Th}\ L} = \frac{30}{1.9 \times 10^8 * 8} = 2 \times 10^{-8}\ cm/W$$

This value is about a factor of 5 larger than the value deduced from wavelength scaling of that reported by Bloembergen (Ref. 4) at Ruby wavelengths (see Figure 12). Since the theoretical wavelength scaling for the SRS cross section is fairly straightforward, our results suggest that Bloembergen's reported value is too low. For this blue-green application, our measured small signal gain suggests that this overall Raman approach is relatively easier to accomplish than we had projected in our proposal last year.

The input energy for efficient conversion was also determined from these experiments and the intensity length product needed to accomplish significant conversion was found to be near 3.8×10^9 W/cm. This suggests that an XeF* laser having output near 10 J/cm^2 in a 1 μs pulse would require (for similar H_2 densities) a path length of 3.8 m for efficient conversion to first Stokes to occur--a very practical value.

These calculations do represent approximations however, since, for example, the laser output is in two separate lines and the measured threshold energy, beam waist, conversion length, etc. introduce some additional degree of uncertainty. Further measurements to better establish these values are in progress.

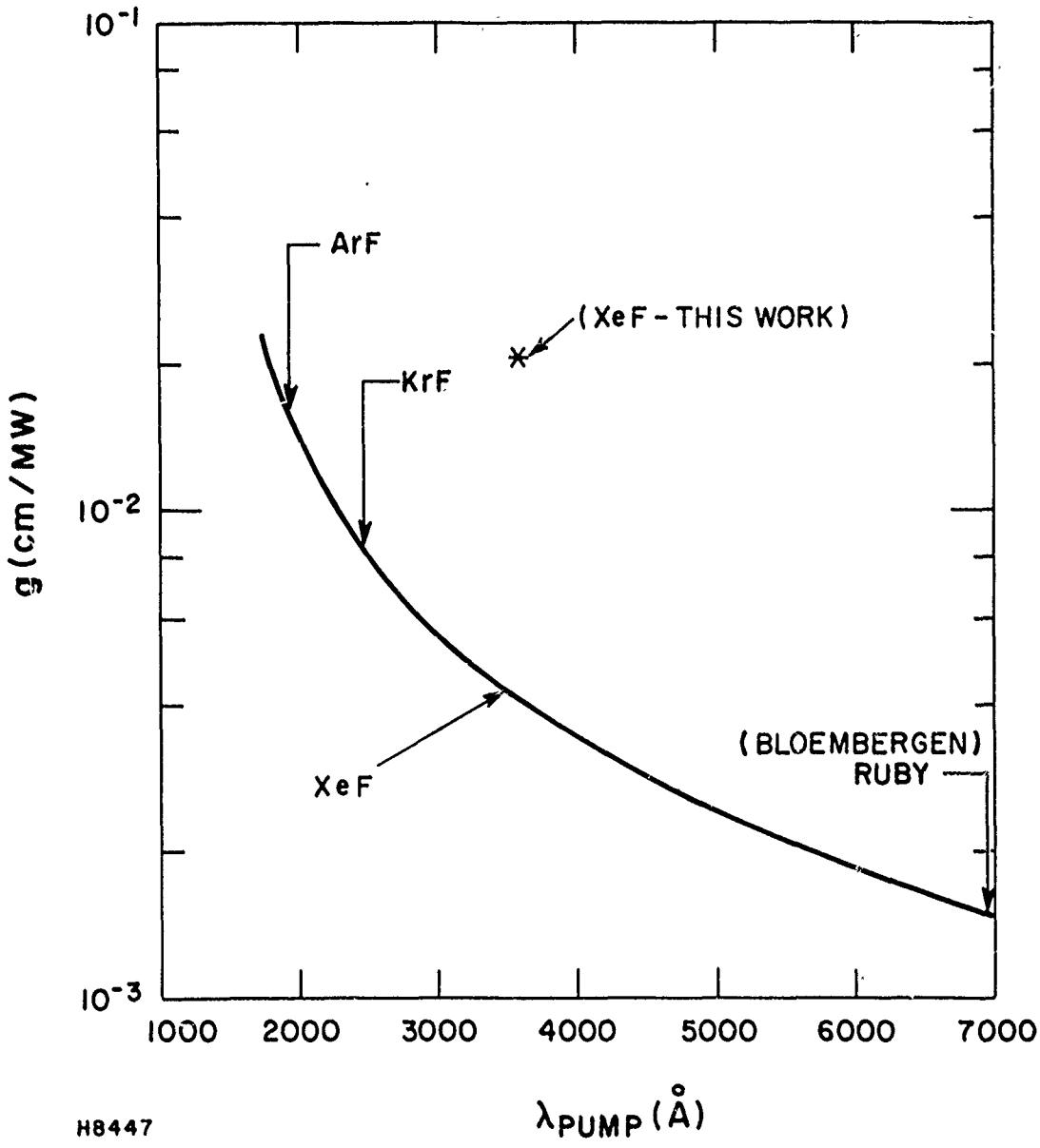

Figure 12 First Stokes Gain for Forward SRS in H_2. Solid line is wavelength-scaled calculation normalized to Bloembergen's result with ruby; *indicates the value deduced from this work.

As mentioned above, this pump laser does produce output at both 3511 Å and 3532 Å (see Figure 13) with ~80% at 3511 Å. The total temporal pulsewidth was measured to be 6 ns (FWHM). When these spectral lines were observed independently with a monochromater, their individual pulsewidths were still near 6 ns but the 353 nm line was delayed slightly from the 351 nm line. This observation is consistent with the observations of others of higher gain in the 351 nm band at room temperature (Ref. 5). Pulse shape measurements of the first Stokes pulses were initially performed with the experimental setup using the 50 cm focus (see Figure 8) at pressures of 10 atm. Characteristic pulse shapes are shown in Figure 14. The top traces show the input laser pulse with the 351, 353 nm XeF lines unresolved. The bottom traces are of the corresponding 410, 413 nm first Stokes lines. The temporal widths of these Stokes-shifted lines are ~4 ns. Similar effects were observed for the softer focus. Measurements of the pulse shape of the second Stokes component from a single cell did not show any further pulse distortion, i.e., they had essentially the same 4 ns pulsewidth as the first Stokes.

All of these data and the above discussion allows us to summarize the results of our single pass, single cell, XeF* pumped H_2 conversion efficiencies for optimized experimental conditions. Conversion efficiencies were calculated by measuring the output energy from the Raman cell through a series of spectral filters, then adjusting the recorded energy for the known transmission of the filters and finally ratioing it to that measured through an empty cell. A photon conversion efficiency of 100% is usually not achievable in these non-resonant molecular Raman systems because as the first Stokes radiation approaches high intensities, it itself acts as a pump and is converted to higher order Stokes emission. Table II contains a summary of the typical output and conversions observed. The

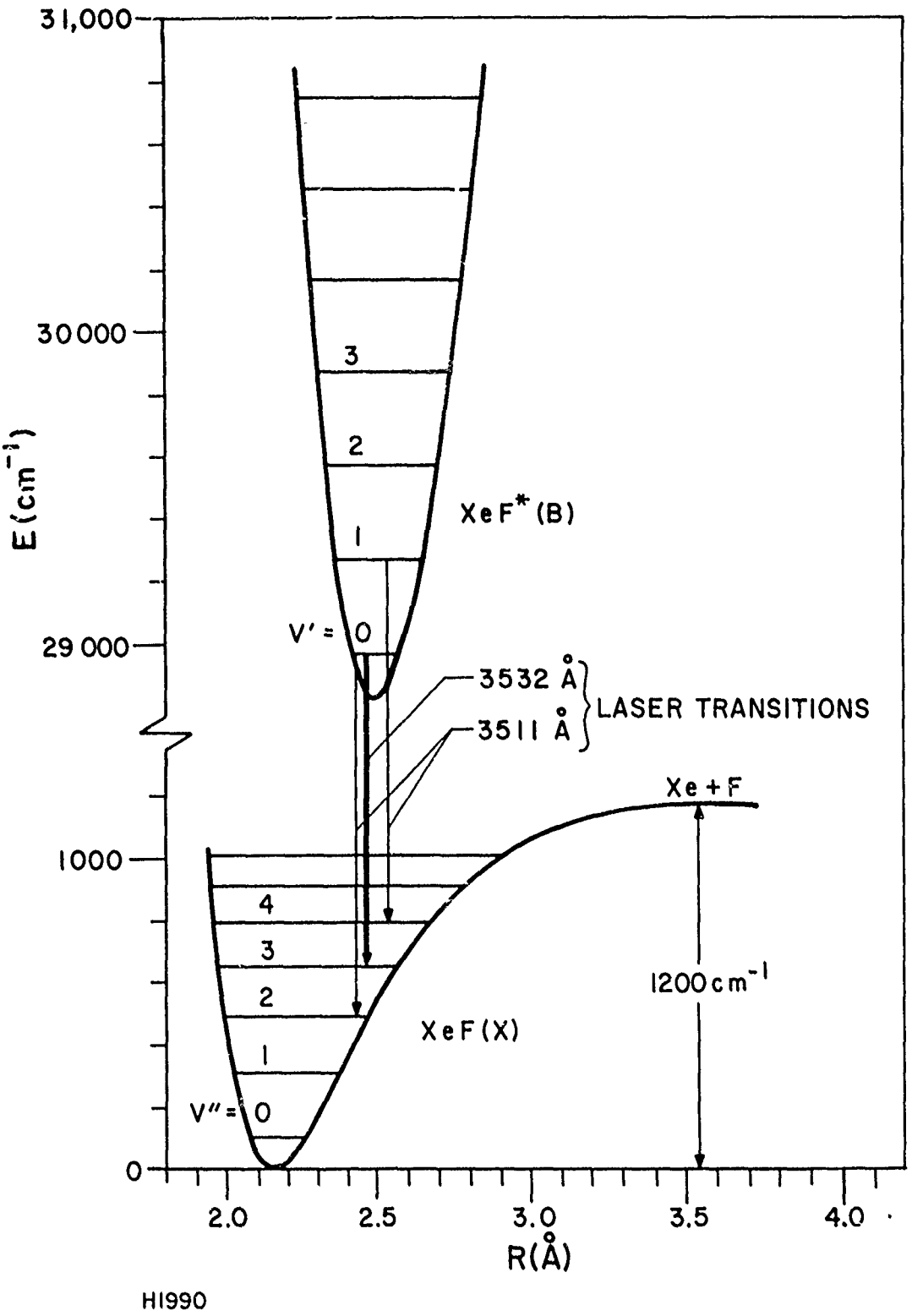

Figure 13 XeF Lasing Transitions

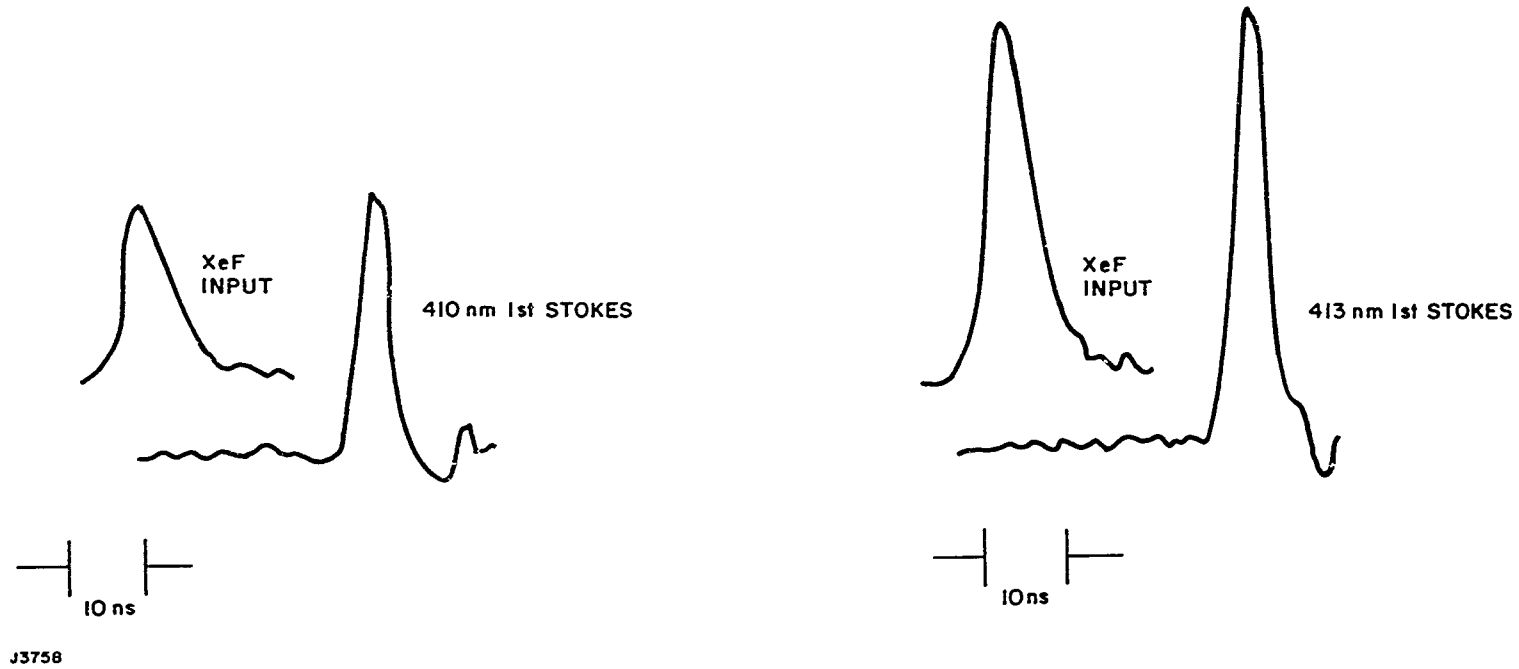

Figure 14 Temporal Characteristics of First Stokes (H_2) Spectral Lines Using the Short Focal Geometry

TABLE II

SUMMARY OF SINGLE CELL XeF-PUMPED H_2 SRS CONVERSION EFFICIENCIES

Pump	Focus	E_{in} (mJ)	E_{out} (mJ)	Energy Eff (%)	Photon Eff	Power Eff	Power Photon Eff
XeF	137 cm	9.6	4.2 S_1	44	61	66	76
			~0 S_2				

power conversion efficiency is the relevant value, since the energy efficiency should approach the power efficiency for sufficiently long pulselengths. These reported efficiencies did vary somewhat from experiment to experiment, however, the values presented here were observed routinely. (The actual highest efficiency for conversion to S_1 with H_2 in a single experimental observation was 57% energy and 86% power conversion efficiency.)

Other stimulated Raman conversion efficiencies for H_2 reported in the literature include 20% photon efficiency into S_1 pumped by a 1.06 μ laser by A. Grasiuk (Ref. 6), while Komine and Stappaerts (Ref. 7), report power photon conversion efficiencies of near 50% into either S_1 or S_2, when H_2 is pumped by a tripled Nd:Yag laser at 355 nm with an oscillator amplifier configuration. Loree, et al. (Ref. 1), have also reported up to 70% energy depletion into various Stokes orders for KrF pumped H_2.

All of these experiments suggest efficient conversion to longer wavelengths via stimulated Raman scattering in a single pass is readily achievable.

The next topic that we addressed in these short pulse, low energy experiments was the second step in the two-step process; namely, investigation of the conversion properties of the emerging S_1 from cell one, subsequently acting as a pump, to produce its S_1 in cell two. (See Figure 15.)

The first of these experiments consisted of two-step shifting through two cells filled with hydrogen, i.e., XeF $\rightarrow$ H_2 $\rightarrow$ H_2. The first cell was optimized for maximum conversion of XeF* to first Stokes, S_1, at 410, 413 nm. These emerging laser photons were separated from the depleted pump via a dielectric coated mirror. The depleted XeF* pump was thus rejected, while the first Stokes beam from cell one was focussed into the second cell, also optimized to convert into its own first Stokes at 495 nm and 499 nm.

2 CELL EXPERIMENTS

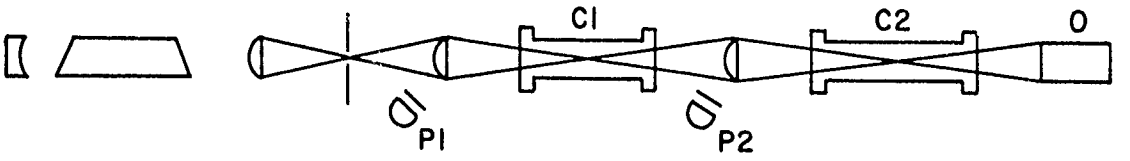

J3735

Figure 15 Schematic of Experimental Setup where C_1 and C_2 are the Two High-Pressure Cells and P_1, P_2 the Photodiodes for Monitoring the Inputs to each Cell Respectively

Experimentally, the same conversion efficiencies observed through the first cell were not observed in the second step. This was essentially due to the limitations in S_1 energies (acting as the pump) which could be delivered into the second cell through the various optical components (mirror, lens, window, etc.). We were apparently just over threshold in pump laser intensity for the second-step SRS process.

Specifically, the XeF pump laser was focussed into the first cell with a focal length of about 135 cm and the cell was maintained at pressures > 40 atm to insure good conversion. The output light (depleted XeF* and S_1 radiation) resulting from this optimized configuration was collected and then refocussed into a second cell. A dielectric coated mirror was usually employed, behind the first cell, to reflect (> 99.9%) of the depleted pump yet partially transmit (~ 50%) the first Stokes radiation. The waist diameter and conversion length of this S_1 radiation was measured as before (see Figure 16). From this figure, the effective gain length is near 5 cm and the power density at the focus is estimated as follows:

0.05 cm pinhole

$$\frac{1.5 \times 10^{-3}\ \text{J}}{4 \times 10^{-9}\ \text{s}} \quad \frac{4}{\pi (0.05)^2\ \text{cm}^2} = 1.9 \times 10^8\ \frac{\text{W}}{\text{cm}^2}$$

0.04 cm pinhole

$$\frac{0.7 \times 10^{-3}\ \text{J}}{4 \times 10^{-9}} \quad \frac{4}{\pi (0.04)^2 \text{cm}^2} = 1.4 \times 10^8\ \frac{\text{W}}{\text{cm}^2}$$

This represents a lower limit for the actual power density of this first Stokes laser light in that $\gtrsim$ 50% of the power was lost in transmission through the optical components. When these are taken into account, the measured power density of the first Stokes compares favorably with the XeF pump (4.5×10^8 W/cm^2) and indicates that the beam quality of the emerging Raman Stokes shifted light is comparable to the pump.

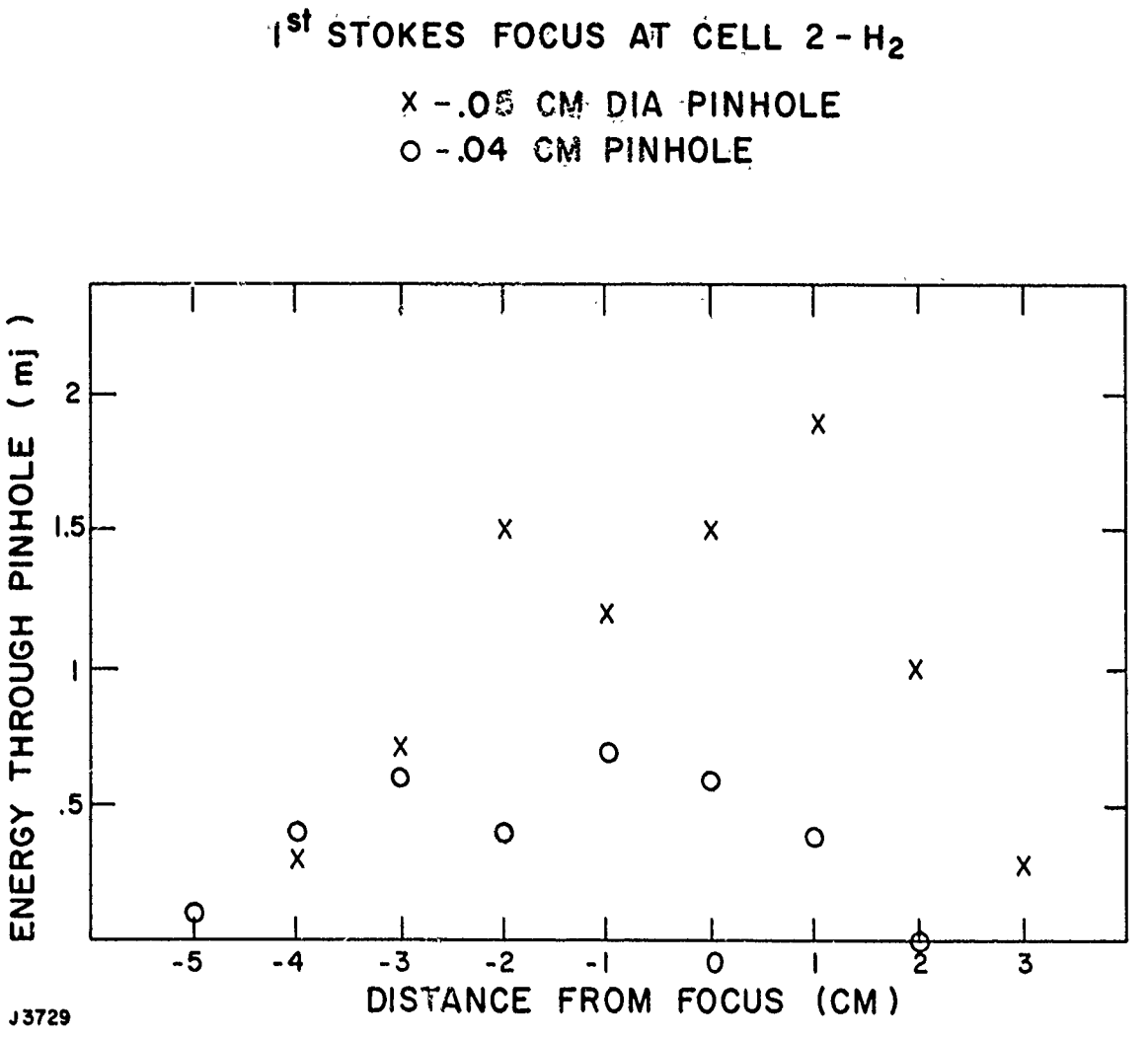

Figure 16 Energy Measured Through 0.05 or 0.04 cm Diameter Pinholes vs Distance from Focus for S_1 Radiation

The variation of the conversion features with the pressure in the second cell was qualitatively similar to that measured in the single cell experiments. Figure 17 shows a plot of the output as measured with the OMA when the pressure in the second cell was varied. (These data are not directly comparable in that the sensitivity of the OMA is greater at 500 nm than at 400 nm but the degree is unknown.) The points at "zero pressure" indicate that the input consisted of both S_1 and S_2.

Threshold in the second cell was measured by monitoring the first Stokes input with a photodiode and the second Stokes output with another photodiode. The results are summarized in Figure 18. In these experiments, the first Stokes, acting as a pump in the second cell, is probably not far above threshold.

The intensity-length product for conversion of $XeF^*/H_2/H_2$ can be calculated from these second-cell experiments. The threshold energy was near 1 mJ. The pulselength was 4 ns with a beam waist of 0.05 cm and a conversion length $\sim$5 cm at the focus of the second cell. The intensity-length product is, therefore, near 6×10^8 W/cm which is considerably less (even after wavelength scaling is accounted for in the calculation) than the value calculated from the single-cell experiments. This lowered (apparent) threshold is caused by the presence of a small amount of second Stokes radiation emitted from cell 1 and entering into cell 2. This small amount of second Stokes can act as the initial input for the conversion process and would require less amplification (i.e., a total gain significantly < 30) for stimulated Raman scattering to occur.

The temporal features of the two-step conversion are depicted in Figure 19. This figure shows the XeF pump, the first Stokes output of cell 1 and the second Stokes output of cell 2, when both cells were filled with H_2. The pulsewidth goes from 6 ns for the XeF laser to 4 ns for S_1 to 2.5 ns (FWHM) for S_2, although the general pulse shapes remained the same.

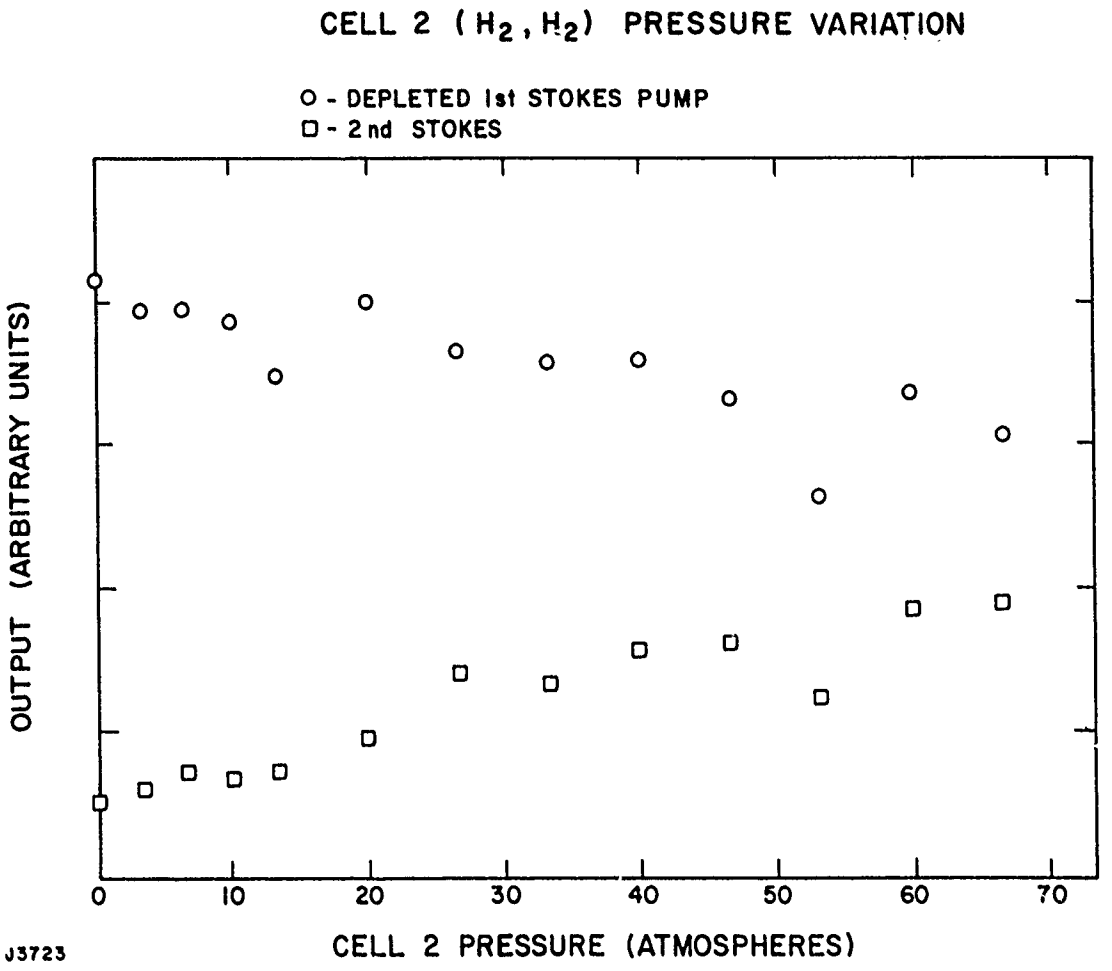

Figure 17 Cell 2 (H_2, H_2) Pressure Variation Effect on S_1 Pump and the Generation of S_2

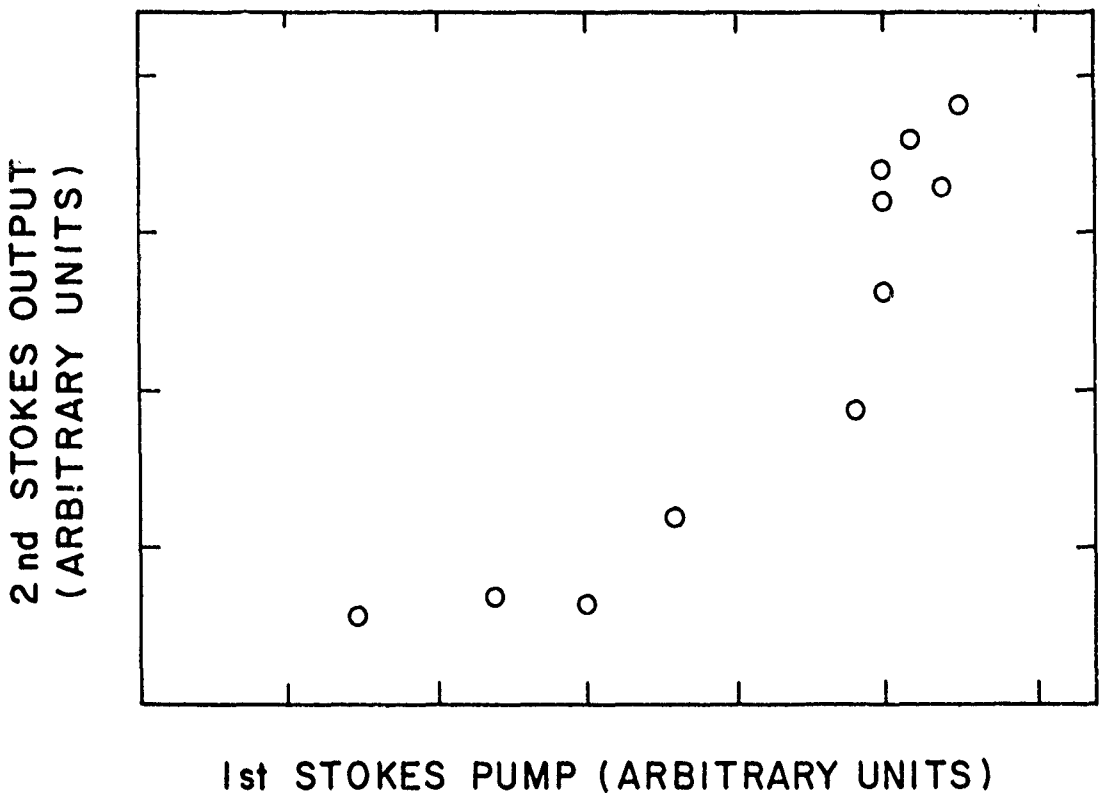

Figure 18 Cell 2 Threshold for S_2 as a Function of S_1 Input Intensity

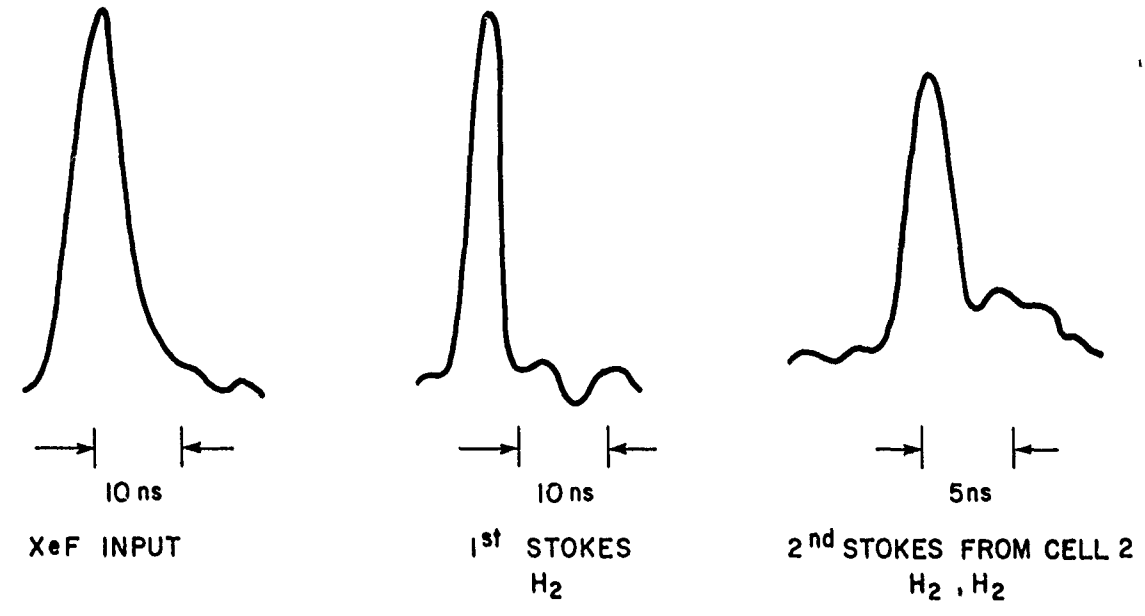

Figure 19 Pulse Temporal Narrowing in Successive Conversion

The typical energy conversion efficiency measured in this manner was 25 to 30% into S_2 output from the S_1 input, i.e., 495 out/410 in. This corresponds to a photon conversion efficiency of 30 to 35%, a power efficiency due to pulse shortening of 40 to 48% and a photon power efficiency of 48 to 56%. The total energy conversion efficiency from the XeF input into cell 1 into S_2 output from cell 2 was 12% (34% photon power conversion). As discussed above, conversion efficiency characteristics of what was achieved in a single cell should be achievable in any subsequent cell for an overall conversion of $\eta_1\eta_2$. Since we measured power conversion efficiencies of 66% in a single cell, overall conversion > 40% to the blue-green should be achievable, but were unobtainable here due to the low pump intensities available.

This conjecture was tested somewhat by conducting two-step experiments with KrF* as the pump. The KrF laser operates at higher output intensities and was capable of generating significant quantities of S_1 through D_2 (see Figure 20). In this case, the first cell contained 67 atm of D_2 which resulted in an output consisting mainly of depleted pump (249 nm) and S_1 at 268 nm. These laser transitions were collected and focussed into the second cell containing H_2. They each generated their own Stokes components in cell 2 but, most of the output consisted of a few first Stokes orders (see Figure 20). Of particular interest is the fact that the 268 nm S_1 output of cell 1 was depleted over 70% in cell 2, with the majority of the output appearing in the sought after 308 nm line (which would be analogous to the production of 469 and 472 with XeF as the pump).

B. LONG PULSE EXPERIMENTS

Included as part of this DARPA-supported program, we also investigated Raman scattering using the output of a one-meter laser as the pump for single pass, single cell spectral observations. To perform these experiments, two different e-beam

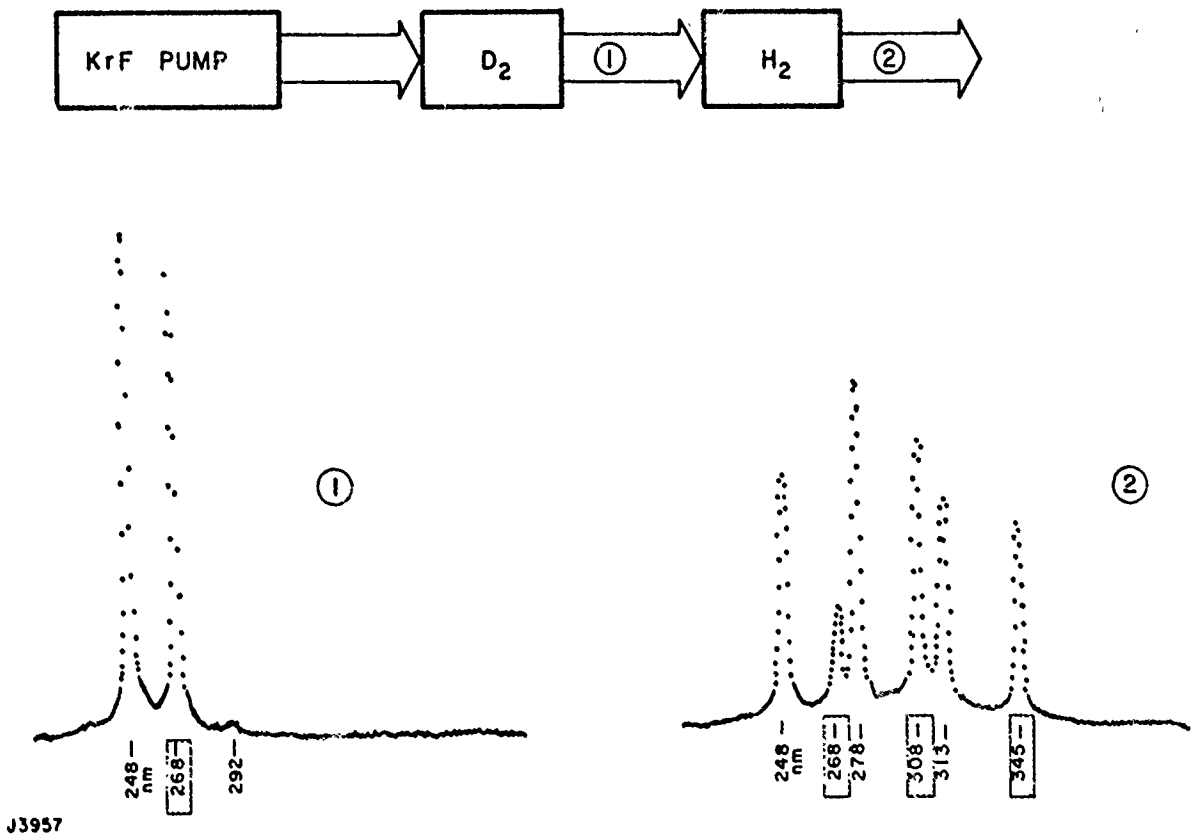

Figure 20 Two Step KrF/D_2/H_2 Raman Conversion

laser devices were used. The first experiments which were carried out last summer involved the (10 x 10 x 100) cm^3 device constructed in support of the N00014-76-C-1032 DARPA-funded contract. It was run with conventional optics and provided ~ 5 J in 600 ns for the few experiments we tried. Under these conditions, the output was collected by a 6-in. Ultrasil quartz plano-convex lens (50 cm fl) and focused into the center of our high pressure H_2 cell (~ 10 atm). We observed output spectra corresponding to S_1, S_2 and AS_1 (see Figure 21). From color Polaroid open shutter photographs, it appeared that the output consisted of principally parametric four-wave conversion processes as was evidenced by the observation of annular rings. Also, the intensity correlations in the Stokes radiation ($AS_1 > S_2$) supported this contention.

More recently, we performed SRS experiments using a (2 x 2 x 100) cm^3 e-beam device operating with KrF* at 249 nm. This device produced ~ 0.5 J in 0.3 μs with flat (stable) optics. This output was again focussed into the high-pressure H_2 cell (> 30 atm) and significant conversion to S_1, S_2 and some S_3 was observed using the OMA (see Figure 22). Energy measurements showed energy conversion to these Stokes lines was significantly > 10%. Also, photodiode measurements of the pump pulse and first Stokes pulse showed conversion occurred over the entire extended pulselength (see Figure 23). We believe the temporal features seen in the Raman output represent amplification of small-scale temporal structure in the laser pump due to the many cavity modes present in the stable optics (flat-flat) setup.

This cavity has been modified to include Brewster windows and unstable optics (see Figure 24). Energy output near 0.6 J in 0.4 s has been routinely observed. Using this beam, we have observed long pulselength XeF* SRS in H_2 (see Figure 25). Here the OMA shows conversion is principally into S_1 (413 nm) with significant depletion of the XeF pump and generation of S_2 (499 nm). These data are not calibrated and these

LONG PULSE LENGTH XeF* SRS EXPERIMENT
(10 ATM H_2)

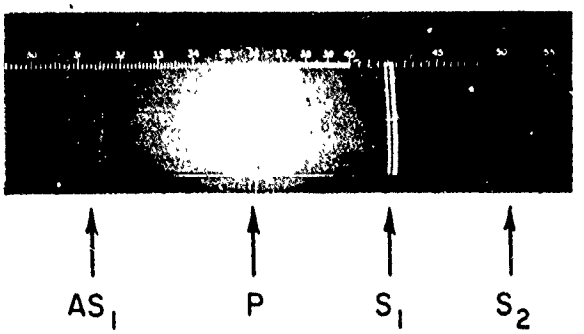

J3827

Figure 21 Spectra Giving Qualitative Indication of Relative Intensities of XeF Pumped H_2 (AS_1, P, S_1, S_2)

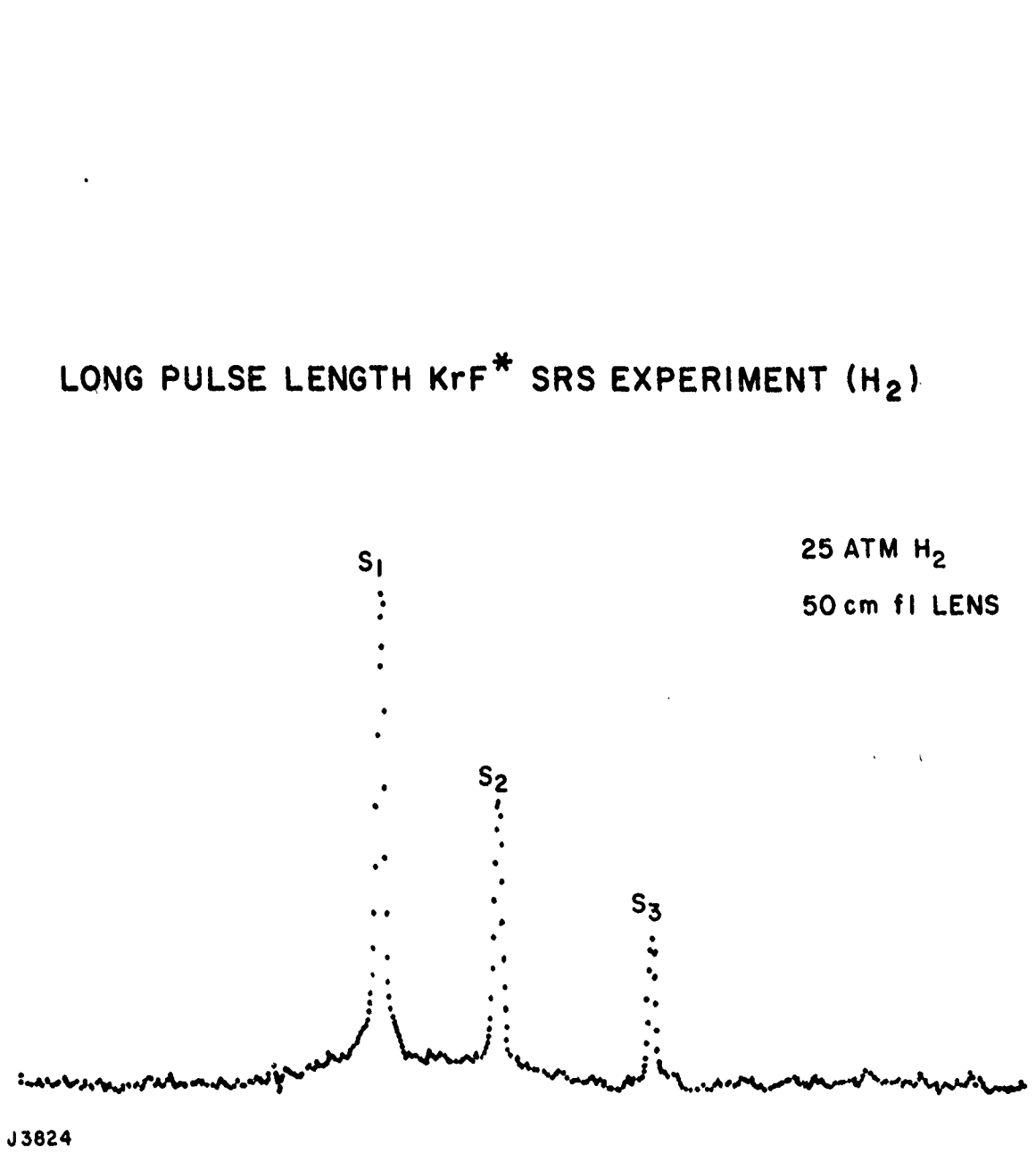

Figure 22 OMA Output for KrF Pumped H_2 with Filter to Remove Pump (249 nm) and Shorter Wavelengths

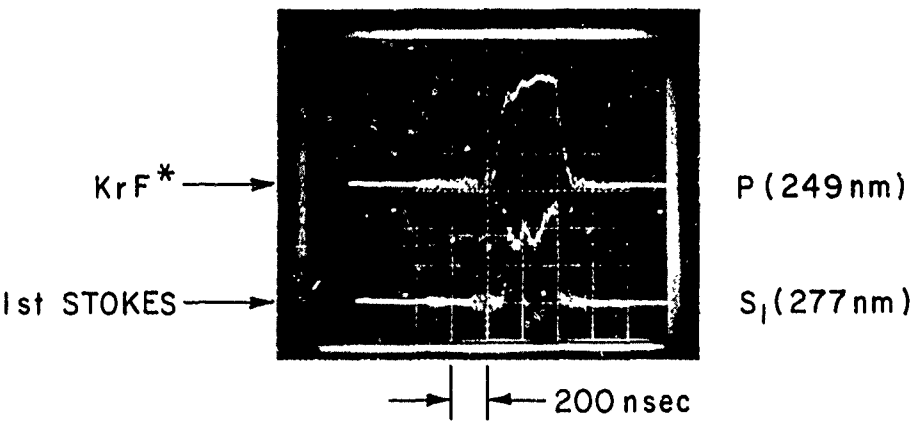

Figure 23 Temporal Pulse Shapes of Input KrF Pump and S_1 Stokes Shifted Raman Pulse

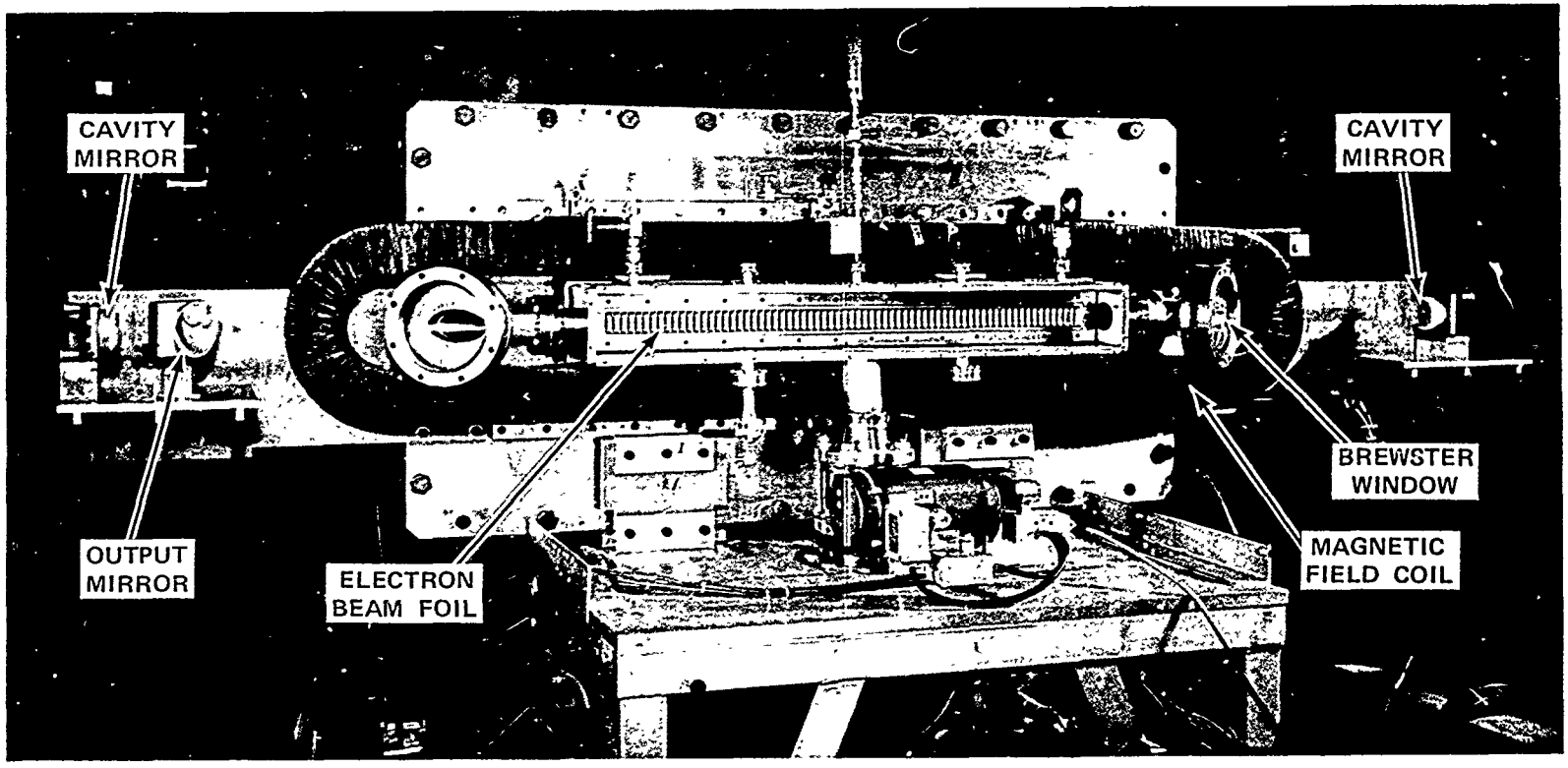

J3829

Figure 24 Photograph of Modified One Meter Laser

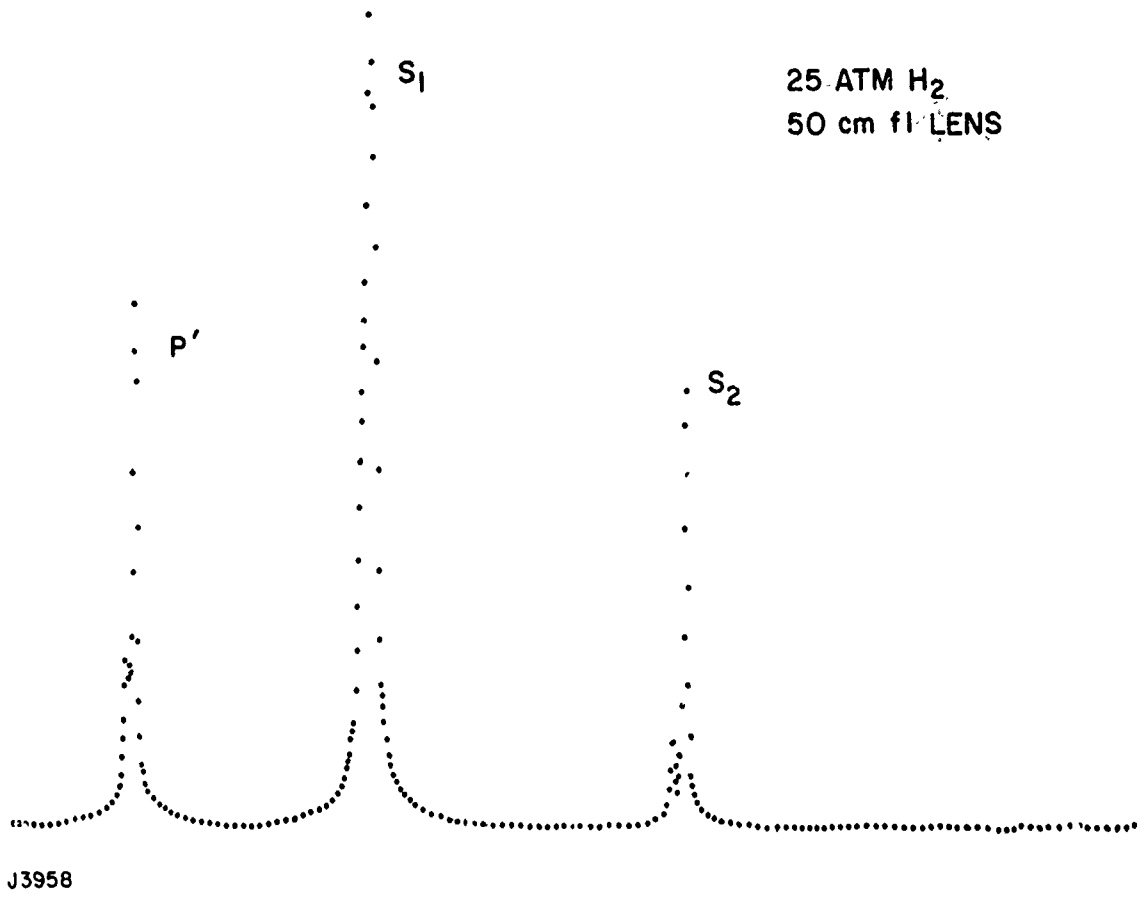

Figure 25 Long Pulse Length XeF* SRS Experiment (H_2)

spectral results are merely qualitative. More quantitative results are shown in Figure 26 where the XeF pump was softly focused (~ 135 cm) into about 30 atm H_2. Data collected with photodiodes and appropriate filters showed ~ 35% pump depletion with the majority going into first stokes in good agreement with our expectations. These conversion experimental results are preliminary. Further experimentation is underway and will be summarized in subsequent Interim Technical Reports.

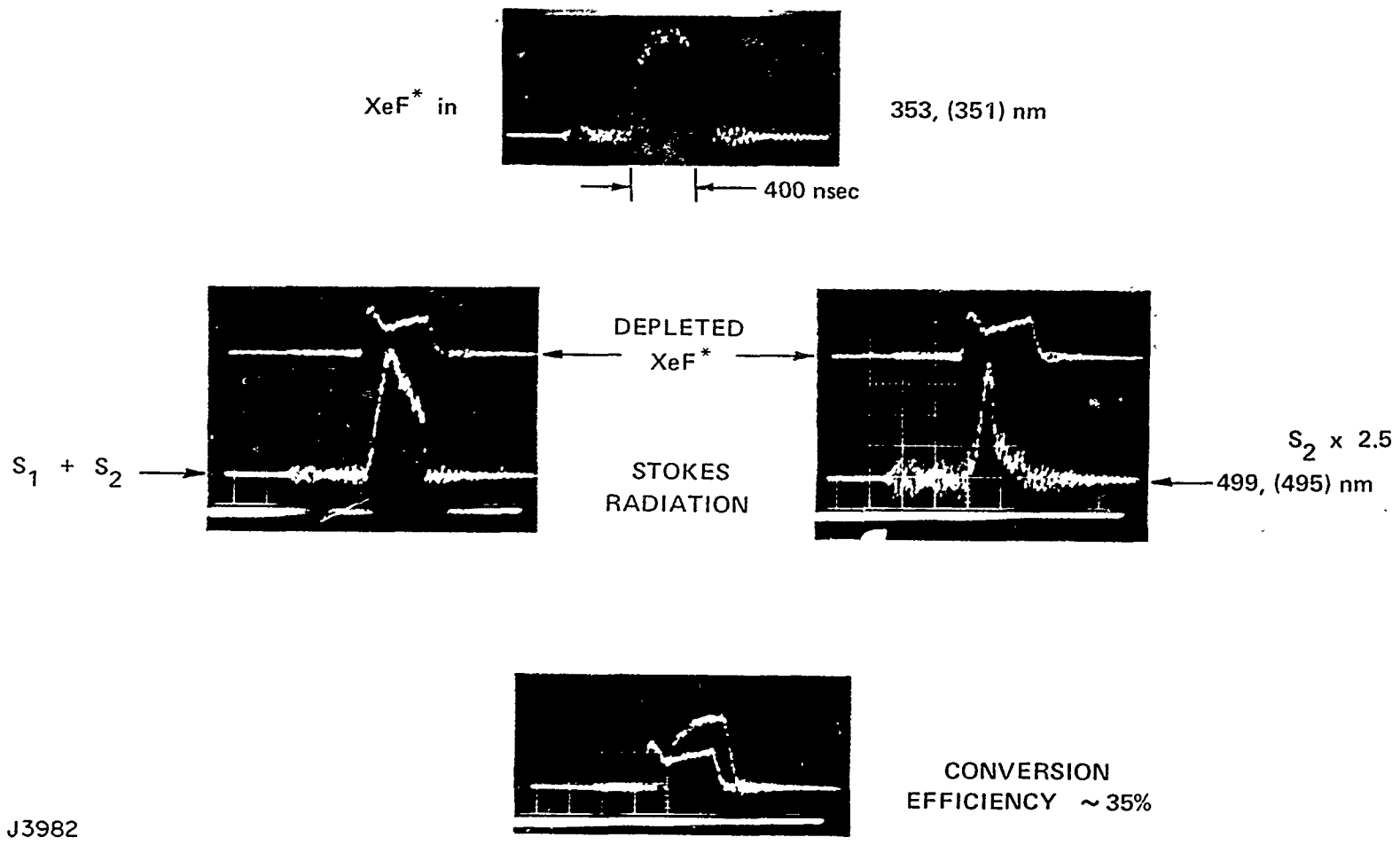

Figure 26 XeF* Pumped SRS Experiment (H_2) (One Meter Device)

REFERENCES

1. Loree, T.R., Sze, R.C. and Barker, D.L., App. Phys. Lett. 31, 37 (1977).

2. Burnham, R., Strategic Blue-Green Optical Communications Program, Arlington, VA (17 May 1974).

3. Barker, D.L. and Loree, T.R., Appl. Opt. 16, 1192 (1977).

4. Bloembergen, H., Bret, G., Lallemand, P., Pine, A. and Simova, P., IEEE J. Quant. Electron 3, 197 (1967).

5. Goldhar, J., Dickie, J., Bradley, L.P. and Pleasance, L.D., App. Phys. Lett. 31, 677 (1977).

6. Grasiuk, A., Private Communication (Dec. 1978).

7. Komine, H. and Stappaerts, E.A., Optics Lett. 4, 348 (1979).

DISTRIBUTION LIST

Office of Naval Research, Department of the Navy, Arlington, VA 22217 - Attn: Physics Program (1 copy)

Naval Research Laboratory, Department of the Navy, Washington, D.C. 20375 - Attn: Technical Library (1 copy)

Office of the Director of Defense, Research and Engineering, Information Office Library Branch, The Pentagon Washington, D.C. 20301 - (1 copy)

U.S. Army Research Office, Box CM, Duke Station, Durham, N.C. 27706 - (1 copy)

Defense Documentation Center, Cameron Station, Alexandria, VA 22314 - (1 copy)

Defender Information Analysis Center, Battelle Memorial Institute, 505 King Avenue, Columbus, OH 43201 - (1 copy)

Commanding Officer, Office of Naval Research Branch Office, 536 South Clark Street, Chicago, IL 60615 - (1 copy)

New York Area Office, Office of Naval Research, 715 Broadway (5th Floor), New York, NY 10003 - Attn: Dr. Irving Rowe (1 copy)

Air Force Office of Scientific Research, Department of the Air Force, Washington, D.C. 22209 - (1 copy)

Office of Naval Research Branch Office, 1030 East Green Street, Pasadena, CA 91106 - Attn: Dr. Robert Behringer (1 copy)

Defense Advanced Research Projects Agency, 1400 Wilson Blvd., Arlington, VA 22209 - Attn: Strategic Technology Office (1 copy)

Office Director of Defense, Research and Engineering, The Pentagon, Washington, D.C. 20301 - Attn: Asst. Dir. (Space and Adv. Systems) (1 copy)

Office of the Assistant Secretary of Def., System Analysis (Strategic Programs), Washington, D.C. 20301 - Attn: Mr. Gerald R. McNichols

U.S. Arms Control and Disarmament Agency, Dept. of the State Bldg., Rm. 4931, Washington, D.C. 20451 Attn: Dr. Charles Henkin - (1 copy)

Energy Research Development Agency, Division of Military Applications, Washington, D.C. 20545 - (1 copy)

National Aeronautics and Space Admin., Lewis Research Center, Cleveland, Oh 44135 - Attn: Dr. John W. Dunning, Jr. Aerospace Research Engineer (1 copy)

National Aeronautics & Space Admin., Code RR, FOB 10B, 600 Independence Ave., SW, Washington, D.C. 20546 - (1 copy)

National Aeronautics and Space Admin., Ames Research Center, Moffit Field, CA 94035 - Attn: Dr. Kenneth W. Billman (1 copy)

Department of the Army, Office of the Chief of RD&A, Wshington, D.C. 20310 - Attn: DARD-DD (1 copy)

Department of the Army, Office of the Chief of RD&A, Washington, D.C. 20310 - Attn: DAMA-WSM-T (1 copy)

Department of the Army, Office of the Deputy Chief of Staff for Operations and Plans, Washington, D.C. 20310 Attn: DAMO-RQD (1 copy)

U.S. Army Missile Command, Research and Development Division, Redstone Arsenal, AL 35809 - Attn: Army High Energy Laser Programs (1 copy)

Commanding Officer, U.S. Army Mobility Equipment R&D Center, Ft. Belvoir, VA 22060 - Attn: SMEFB-MW (1 copy)

Commander, U.S. Army Armanent Command, Rock Island, IL 61201 - Attn: AMSAR-RDT (1 copy)

Director, Ballistic Missile Defense Adv. Technology Center, P.O. Box 1500, Huntsville, AL 35807 - Attn: ATC-O (1 copy)

Director, Ballistic Missile Defense Adv. Technology Center, P.O. Box 1500, Huntsville, AL 35807 - Attn: ACT-T

Commanding General, U.S. Army Munitions Command, Dover, NH 17801 - Attn: Mr. Gilbert F. Chesnov (AMSMU-R) (1 copy)

Director, U.S. Army Ballistics Res. Lab., Aberdeen Proving Ground, MD 21005 - Attn: Dr. Robert Eichenberger (1 copy)

Commandant U.S. Army, Air Defense School, Ft. Bliss, TX 79916 - Attn: Air Defense Agency (1 copy)

Commandant, U.S. Army, Air Defense School, Ft. Bliss, TX 79916 - Attn: ATSA-CTD-MS (1 copy)

Commanding General, U.S. Army Combat Dev. Command, Ft. Belvoir, VA 22060 - Attn: Director of Material, Missile Div. (1 copy)

Commander, U.S. Army Training and Doctrine Command, Ft. Monroe, VA 23651 - Attn: ATCD-CF (1 copy)

Commander, U.S. Army Electronics Command, Ft. Monmouth, NJ 07703, Attn: AMSEL-CT-L, Dr. R.G. Buser (1 copy)

Commander, U.S. Army Combined Arms Combat Dev. Act., Ft. Leavenworth, KS 66027 - (1 copy)

National Security Agency, Ft., Gec. G. Meade, MD 20755 - Attn: R.C. FOSS A763 (1 copy)

Deputy Commandant - For Combat and Training Developments, U.S. Army Ordnance Center and School, Aberdeen Proving Ground, MD 21005 - Attn: ATSL-CTD-MS-R (1 copy)

Department of the Navy, Office of the Chief of Naval Operations, The Pentagon 50739, Washington, D.C. 20350 - Attn: (OP 982F3)

Boston Branch Office, Bldg. 114, Section D, 666 Summer Street, Boston, MA 02210 (1 copy)

Department of the Navy, Deputy Chief of Navy Material (Dev.), Washington, D.C. 20360 - Attn: Mr. R. Gaylord (MAT 032B) (1 copy)

Naval Missile Center, Point Mugu, CA 93042 - Attn: Gary Gibbs (Code 5352) (1 copy)

Naval Research Laboratory, Washington, D.C. 20375 - Attn: Electro Optical Technology, Program Office, Code 1409 (1 copy)

Naval Research Laboratory, Washington, D.C. 20375 - Attn: Dr. P. Livingston - Code 5560 (1 copy)

Naval Research Laboratory, Washington, D.C. 20375 - Attn: Dr. A.I. Schindler - Code 6000 (1 copy)

Naval Research Laboratory, Washington, D.C. 20375 - Attn: Dr. John L. Walsh - Code 5503 (1 copy)

High Energy Laser Project Office, Department of the Navy, Naval Sea System Command, Washington, D.C. 20360 - Attn: Capt. A. Skolnick, USN (PM 22) (1 copy)

Superintendent, Naval Postgraduate School, Monterey, CA 93940 - Attn: Library (Code 2124) (1 copy)

Navy Radiation Technology, Air Force Weapons Lab (NLO), Kirtland AFB, NM 87117 (1 copy)

Naval Surface Weapons Center, White Oak, Silver Spring, MD 20910 - Attn: Dr. Leon H. Schindel (Code 310) (1 copy)

DISTRIBUTION LIST (Continued)

Naval Surface Weapons Center, White Oak, Silver Spring, MD 20910 - Attn: Dr. E. Leroy Harris (Code 313) (1 copy)
Naval Surface Weapons Center, White Oak, Silver Spring, MD 20910 - Attn: Mr. K. Enkenhaus (Code 034) (1 copy)
Naval Surface Weapons Center, White Oak, Silver Spring, MD 20910 - Attn: Mr. J. Wise (Code 047) (1 copy)
Naval Surface Weapons Center, White Oak, Silver Spring, MD 20910 - Attn: Technical Library (1 copy)
U.S. Naval Weapons Center, China Lake, CA 93555 - Attn: Technical Library (1 copy)
HQ AFSC/XRLW, Andrews AFB, Washington, D.C. 20331 - Attn: Maj. J.M. Walton (1 copy)
HQ AFSC (DLCAW), Andrews AFB, Washington, D.C. 20331 - Attn: Maj. H. Axelrod (1 copy)
Air Force Weapons Laboratory, Kirtland AFB, NM 87117 - Attn: LR (1 copy)
Air Force Weapons Laboratory, Kirtland AFB, NM 87117 - Attn: AL (1 copy)
HQ Aeronautical Systems Div., Wright Patterson AFB, OH 45433 - Attn: XRF - Mr. Clifford Fawcett (1 copy)
Rome Air Development Command, Griffiss AFB, Rome, NY 13440 - Attn: Mr. R. Urtz (OCSE) (1 copy)
HQ Electronics Systems Div. (ESL), L.G. Hanscom Field, Bedford, MA 01730 - Attn: Mr. Alfred E. Anderson (XRT) (1 copy)
HQ Electronics Systems Div. (ESL), L.G. Hanscom Field, Bedford, MA 01730 - Attn: Technical Library (1 copy)
Air Force Rocket Propulsion Lab., Edwards AFB, CA 93523 - Attn: B.R. Bornhorst, (LKCG) (1 copy)
Air Force Aero Propulsion Lab., Wright Patterson AFB, OH 45433 - Attn: Col. Walter MOE (CC) (1 copy)
Dept. of the Air Force, Foreign Technology Division, Wright Patterson AFB, OH 45433 - Attn: PDTN (1 copy)
Commandant of the Marine Corps., Scientific Advisor (Code RD-1), Washington, D.C. 20380 (1 copy)
Aerospace Research Labs., (AP), Wright Patterson AFB, OH 45433 - Attn: Lt. Col. Max Duggins (1 copy)
Defense Intelligence Agency, Washington, D.C. 20301 - Attn: Mr. Seymour Berler (DTIB) (1 copy)
Central Intelligence Agency, Washington, D.C. 20505 - Attn: Mr. Julian C. Nall (1 copy)
Airesearch Maunuf. Co., 9851-9951 Sopulveda Blvd., Los Angeles, CA 90009 - Attn: Mr. A. Colin Stancliffe (1 copy)
Atlantic Research Corp., Shirley Highway at Edsall Road, Alexandria, VA 22314 - Attn: Mr. Robert Naismith (1 copy)
Battelle Columbus Laboratories, 505 King Avenue, Columbus, OH 43201 - Attn: Mr. Fed Tietzel (STPIAC) (1 copy)
Bell Aerospace Co., Buffalo, NY 14240 - Attn: Dr. Wayne C. Solomon (1 copy)
Boeing Company, P.O. Box 3999, Seattle, WA 98124 - Attn: Mr. M.I. Gamble (2-,460,MS 8C-88) (1 copy)
Electro-Optical Systems, 300 N. Halstead, Pasadena, CA 91107 - Attn: Dr. Andrew Jensen (1 copy)
General Electric Co., Space Division, P.O. Box 8555, Philadephia, PA 19101 - Attn: Dr. R.R. Sigismonti (1 copy)
General Electric Co., 100 Plastics Avenue, Pittsfield, MA 01201 - Attn: Mr. D.G. Harrington (Rm. 1044) (1 copy)
Hercules, Inc., Industrial Dept., Wilmington, DE 19899 - Attn: Dr. R.S. Voris (1 copy)
Hercules, Inc., P.O. Box 210, Cumberland, MD 21502 - Attn: Dr. Ralph R. Preckel (1 copy)
Hughes Research Labs., 3011 Malibu Canyon Road, Malibu, CA 90265 - Attn: Dr. D. Forster (1 copy)
Hughes Aircraft Co., Aerospace Group-Systems Division, Canoga Park, CA 91304 - Attn: Dr. Jack A. Alcalay (1 copy)
Hughes Aircraft Co., Centinela and Teale Streets, Building 6, MS E-125, Culver City, CA 90230 - Attn: Dr. William Yates (1 copy)
Institute for Defense Analyses, 400 Army-Navy Drive, Arlington, VA 22202 - Attn: Dr. Alvin Schnitzler (1 copy)
Lawrence Livermore Laboratory, P.O. Box 808, Livermore, CA 94550 - Attn: Dr. R.E. Kidder (1 copy)
Lawrence Livermore Laboratory, P.O. Box 808, Livermore, CA 94550 - Attn: Dr. E. Teller (1 copy)
Lawrence Livermore Laboratory, P.O. Box 808, Livermore, CA 94550 - Attn: Dr. Joe Fleck (1 copy)
Los Alamos Scientifc Labortory, P.O. Box 1663, Los Alamos, NM 87544 - Attn: Dr. Keith Boyer (1 copy)
Lockheed Palo Alto Research Lab., 3251 Hanover Street, Palo Alto, CA 94303 - Attn: L.R. Lunsford, Orgn. 52-24, Bldg. 201 (1 copy)
Mathematical Sciences Northwest, Inc., P.O. Box 1887, Bellevue, WN 98009 - Attn: Dr. Abraham Hertzberg (1 copy)
Massachusetts Institute of Technology, Lincoln Laboratory, P.O. Box 73, Lexington, MA 02173 - Attn: Dr. S. Edelberg (1 copy)
Massachusetts Institute of Technology, Lincoln Laboratory, P.O. Box 73, Lexington, MA 02173 - Attn: Dr. L.C. Marquet (1 copy)
McDonnell Douglas Astronautics Co., 5301 Bolsa Avenue, Huntington Beach, CA 92647 - Attn: Mr. P.L. Klevatt, Dept. A3-830-BBFO, M/Sg (1 copy)
McDonnell Douglas Research Labs., Dept. 220, Box 516, St. Louis, MO 63166 - Attn: Dr. D.P. Ames (1 copy)
Dr. Anthony N. Pirri, 30 Commerce Way, Woburn, MA 01801 (1 copy)
Rand Corp., 1700 Main Street, Santa Monica, CA 90406 - Attn: Dr. C.R. Culp/Mr. C.A. Carter (1 copy)
Raytheon Co., 28 Seyon Street, Waltham, MA 02154 - Attn: Dr. F.A. Horrigan (Res. Div.) (1 copy)
Raytheon Co., Boston Post Road, Sudbury, MA 01776 - Attn: Dr. C. Sonnenschien (Equip. Div.) (1 copy)
Raytheon Co., Bedford Labs, Missile Systems Div., Bedford, MA 01730 - Attn: Dr. H.A. Mehlhorn (1 copy)
Riverside Research Institute, 80 West End Street, New York, NY 10023 - Attn: Dr. L.H. O'Neill (1 copy)
Riverside Reserach Institute, 80 West End Street, New York, NY 10023 - Attn: Dr. John Bose (1 copy)

DISTRIBUTION LIST (Continued)

Riverside Reserach Institute, 80 West End Street New York, NY 10023 - Attn: (HPEGL Library) (1 copy)

Rockwell International Corporation, Rocketdyne Division, Albuquerque District Office, 3636 Menaul Blvd., Ne, Suite 211, Albuquerque, NM 87110 - Attn: C.K. Kraus, MGR. (1 copy)

Sandia Corp., P.O. Box 5800, Albuquerque, NM 87115 - Attn: Dr. Al Narath (1 copy)

Stanford Reserach Institute, Menlo Park, CA 94025 - Attn: Dr. F.T. Smith (1 copy)

Science Applications, Inc., 1911 N. Ft. Meyer Drive Arlington, VA 22209 - Attn: L. Peckham (1 copy)

Science Applications, Inc., P.O. Box 328, Ann Arbor, MI 48103 - Attn: R.E. Meredith (1 copy)

Science Applications, Inc., 6 Preston Court, Bedford, MA 01703 - Attn: R. Greenberg (1 copy)

Science Applications, Inc., P.O. Box 2351, La Jolla, CA 92037 - Attn: Dr. John Asmus (1 copy)

Systems Science and Software, P.O. Box 1620, La Jolla, CA 92037 - Attn: Alan F. Klein (1 copy)

Systems Consultants, Inc., 1050 31st Street, NW, Washington, D.C. 20007 - Attn: Dr. R.B. Keller (1 copy)

Thiokol Chemical Corp., Wasatch Division, P.O. Box 524, Brigham City, UT 84302 - Attn: Mr. J.E. Hansen (1 copy)

TRW Systems G oup, One Space Park, Bldg. R-1, Rm. 1050, Redondo Beach, CA 90278 - Attn: Mr. Norman Campbell (1 copy)

United Technologies Research Center, 400 Main Street, East Hartford, CT 06108 - Attn: Mr. G.H. McLafferty (1 copy)

United Technologies Reserach Center, Pratt and Whitney Aircraft Div., Florida R&D Center, West Palm Beach, FL 33402, Attn: Dr. R.A. Schmidke (1 copy)

United Technologies Research Center, Pratt and Whitney Aircraft Div., Florida R&D Center, West Palm Beach, FL 33402, Attn: Mr. Ed Pinsley

Varian Associates, EIMAC Division, 301 Industrial Way, San Carlos, CA 94070 - Attn: Mr. Jack Quinn (1 copy)

Vought Systems Division, LTV Aerospace Corp., P.O. Box 5907, Dallas, TX 75222 - Attn: Mr. F.G. _impson, MS254142 (1 copy)

Westinghouse Electric Corp., Defense and Space Center, Balt-Wash. International Airport, Box 746, Baltimore, MD 21203 - Attn: Mr. W.F. List (1 copy)

Westinghouse Research Labs., Beulah Road, Churchill Boro, Pittsburgh, PA 15235 - Attn: Dr. E.P. Riedel (1 copy)

United Technologies Research, East Hartford, CT 06108 - Attn: A.J. DeMaria (1 copy)

Aireborne Instruments Laboratory, Walt Whitorian Road, Melville, NY 11746 - Attn: F. Pace (1 copy)

General Electric R&D Center, Schenectady, NY 12305 - Attn: Dr. Donald White (1 copy)

Cleveland State University, Cleveland, OH 44115 - Attn: Dean Jack Soules (1 copy)

Exxon Research and Engineering Co., P.O. Box 8 Linden, NJ 07036 - Attn: D. Grafstein (1 copy)

University of Maryland, Department of Physics and Astronomy, College Park, MD 20742 - Attn: D. Currie (1 copy)

Sylvania Electric Products Inc., 100 Fergeson Drive, Montian View, CA 94040 - Attn: L.M. Osterink (1 copy)

North American Rockwell Corp., Autonetics Division, 3370 Miraloma Avenue, Anaheim, CA 92803 - Attn: R. Gudmundsen (1 copy)

Massachusetts Institute of Technology, 77 Massachusetts Avenue, Cambridge, MA 02138 - Attn: Prof. A. Javan (1 copy)

Lockheed Missile & Space Co., Palo Alto Research Laboratories, Palo Alto, CA 94304 - Attn: Dr. R.C. Ohlman (1 copy)

Polytechnic Institute of New York, Rt. 110, Farmingtondale, NY 11735 - Attn: Dr. William T. Walter (1 copy)